NASA Technical Memorandum 4216

A Preliminary Evaluation of an F100 Engine Parameter Estimation Process Using Flight Data

Trindel A. Maine, Glenn B. Gilyard,
and Heather H. Lambert

AUGUST 1990

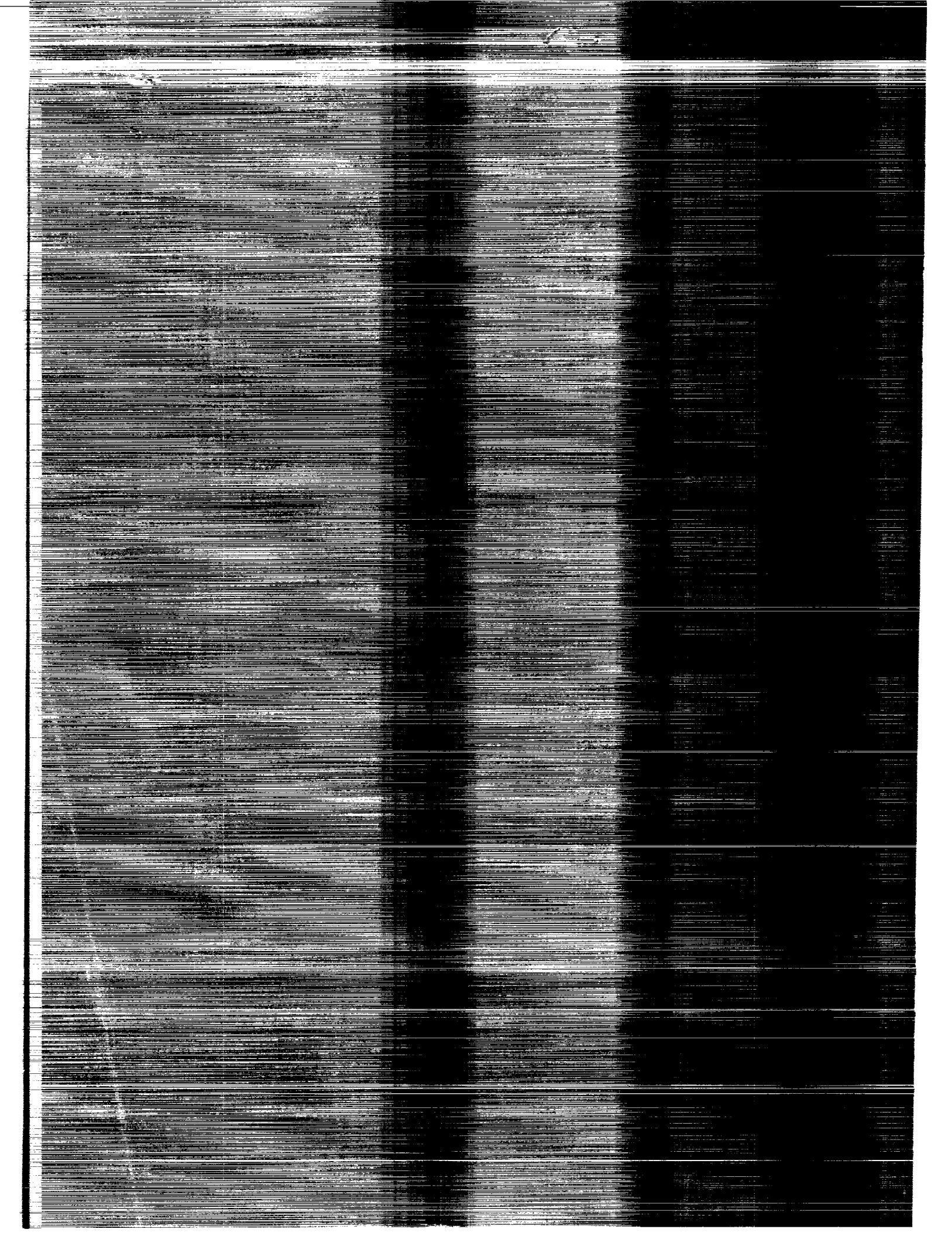

NASA Technical Memorandum 4216

A Preliminary Evaluation of an F100 Engine Parameter Estimation Process Using Flight Data

Trindel A. Maine, Glenn B. Gilyard,
and Heather H. Lambert
Ames Research Center
Dryden Flight Research Facility
Edwards, California

NASA
National Aeronautics and
Space Administration
Office of Management
Scientific and Technical
Information Division
1990

A PRELIMINARY EVALUATION OF AN F100 ENGINE PARAMETER ESTIMATION PROCESS USING FLIGHT DATA

Trindel A. Maine*
Glenn B. Gilyard**
Heather H. Lambert**
NASA Ames Research Center
Dryden Flight Research Facility
Edwards, California

Abstract

The increasing use of digital engine control allows significant improvement in the performance of aircraft engines. This improvement can be achieved by the use of sophisticated control algorithms designed to recover the full performance potential of the propulsion system. The NASA Ames Research Center, Dryden Flight Research Facility; McDonnell Aircraft Company; and Pratt & Whitney are in the process of developing and flight testing a performance seeking control (PSC) system on the NASA F-15 research aircraft to optimize the near-steady-state performance of the F100 turbofan based propulsion system. The paper is a preliminary evaluation of the engine parameter estimation algorithm which is the primary adaptive element of the PSC algorithm. An evaluation has been made using flight data from the F-15 airplane. The flight data presented were obtained at Mach 0.90 and 30,000 ft and at three throttle positions, one of which was at intermediate power. Based on the theoretical formulation and the limited evaluation using flight data, it appears that this estimation algorithm can provide reasonable estimates of an extended set of engine variables needed for advanced propulsion control law development. However, it must be noted that conclusions drawn from this investigation are not strong because of a lack of independent flight measurements of many of the variables being estimated. Additional sensors or independently derived estimates of many of the extended variables are needed to firmly establish the validity of the estimation algorithm.

Nomenclature

A	state matrix
$AAHT$	high pressure turbine area adder deterioration parameter, in^2
AJ	nozzle throat area, in^2
$AJEFF$	effective nozzle throat area, in^2
Ames-Dryden	Ames Research Center, Dryden Flight Research Facility
B	control matrix
BLD	bleed air, lb/sec
C	state observation matrix
CEM	compact engine model
CIVV	compressor inlet variable guide vane angle, deg
D	control observation matrix
DEEC	digital electronic engine control
$DEHPT$	high pressure turbine deterioration parameter, percent
$DELPT$	low pressure turbine deterioration parameter, percent
$DNOZ$	nozzle drag, lbf
$DRAM$	ram drag, lbf
$DWFAN$	fan airflow deterioration parameter, lb/sec

*Aerospace Engineer.
**Aerospace Engineer. Member AIAA.

$DWHPC$	high pressure compressor airflow deterioration parameter, lb/sec
EMD	engine model derivative
F	steady-state model sensitivity matrix
FG	gross thrust, lbf
FNP	net propulsive force, lbf
H_p	pressure altitude, ft
HIDEC	highly integrated digital engine control
HPX	horsepower extraction, lb/sec
K	steady-state Kalman gain matrix
$N1$	fan rotor speed, rpm
$N2$	compressor rotor speed, rpm
P_{amb}	ambient pressure, lb/in^2
PB	burner pressure, lb/in^2
PLA	power lever angle, deg
$PS2$	static pressure at engine face, lb/in^2
PSC	performance seeking control
PT	total pressure, lb/in^2
RCVV	rear compressor variable vanes, deg
SMF	fan stall margin
$SMHC$	high pressure compressor stall margin
SSM	steady-state model
SVM	state variable model
TMT	composite metal temperature
TT	total temperature, °F
$WCFAN$	fan airflow, lb/sec
$WCHPC$	high pressure compressor airflow, lb/sec
WF	gas generator fuel flow, lb/hr
u	control vector
x	state vector
y	vector of estimated engine variables in the steady-state model, and vector of measured variables in the state variable model

Subscripts

b	predicted trim values, interpolated from tables
c	corrected
m	measured
α	angle of attack, deg
β	angle of sideslip, deg

Superscript

$\hat{}$	estimated value of variable

Prefix

Δ	perturbation

Suffix

RES	Kalman filter residuals

Suffix, F100 engine station numbers, ref. Fig.1

2	fan inlet
2.5	compressor inlet
3	compressor discharge
4	high pressure turbine inlet
4.5	low pressure turbine inlet
6	afterburner discharge inlet
7	nozzle throat discharge

Introduction

The increasing use of digital engine control has opened up the possibility of significantly improving the performance of aircraft turbofan engines. This improvement can be achieved by the use of control algorithms designed to recover the full performance potential of the propulsion system. These control algorithms need accurate models of the system and estimates of unmeasured parameters that can be used effectively in a real-time environment over an extended operational envelope. Variations in manufacturing tolerances and the uncertainty associated with engine deterioration and other off-nominal behavior of gas turbine components over time significantly increases the difficulty in developing accurate models.

The Air Force has considerable interest in developing performance seeking control (PSC) technology with the intent of applying it to advanced fighter designs and has funded an independent PSC study.[1] Favorable results from this study support further research into adaptive optimization algorithms. NASA has a history of supporting the development, flight test, and

evaluation of propulsion system improvements. The F-15 flight research program started in the early 1980's by implementing a digital electronic engine control (DEEC)[2,5] followed by flight test of an F100 engine model derivative (EMD),[3] and most recently implementing a highly integrated digital electronic control (HIDEC).[4,6] As an extension of previous NASA propulsion programs and the Air Force PSC study, the NASA Ames Research Center, Dryden Flight Research Facility (Ames-Dryden) contracted for the development of a PSC system on the NASA F-15 research aircraft to optimize the near steady-state performance of an F100 based propulsion system. This system is approaching flight test at NASA Ames-Dryden.

The development of the PSC algorithm has required accurate estimates of variables not normally available on current engines. In preparation for flight test of the NASA PSC program, the contractor developed, Kalman filter based estimation algorithm[7] was evaluated by NASA with flight data obtained during a pre-PSC flight-test phase. Only the estimation portion of the PSC algorithm was evaluated. The estimation algorithm results are significant since the estimation algorithm is not limited in application to the particular control methodology or the specific engine selected for the NASA project. A flight data evaluation of the entire PSC algorithm was not possible prior to actual implementation, because of its closed-loop nature. The algorithm was tested extensively with simulated data during the development process. The simulation results have generally been excellent but are not presented in this paper. The investigation of this paper, using flight data, was made based on the concern that the algorithm may be sensitive to real world problems that are not easily simulated. A particular concern is that the models used in the algorithm were directly derived from the same nonlinear simulation that was used to develop and evaluate the algorithm. Additionally, real data inevitably challenges such simplifying analytical assumptions such as the noise on the system is white or that the engine is operating in steady state.

The parameter estimation algorithm in this paper is a two-step process. The flight evaluation results of each step are presented separately. In the absence of measurements of many of the estimated engine variables, a conclusive evaluation is not possible. However, comparisons are made for a few parameters for which research instrumentation is available but are not normal for production engine instrumentation. The flight data presented were obtained at Mach 0.9 and 30,000 ft altitude and at three throttle positions, one of which was at intermediate power.

Airplane Description

The PSC program will be implemented on the NASA F-15 research airplane which is a high-performance air superiority fighter capable of speeds in excess of Mach 2. The F-15 airplane is powered by two afterburning turbofan F100 engines. The aircraft has been modified with a digital electronic flight control system; the excess capacity of this system is used for the research of integrated propulsion flight control topics. Additional information on the F-15 airplane can be found in Ref. 6.

The F100 EMD engine used in this study is a low-bypass ratio, twin spool, afterburning turbofan derived from the F100-PW-100 engine. The engine incorporates both compressor inlet variable vanes (CIVV) and rear compressor variable vanes (RCVV) to obtain improved performance over a wide range of engine operating conditions. The afterburner consists of a 16-segment augmentor that provides continuously variable thrust augmentation. The convergent–divergent nozzle also has variable area control.

The engine is controlled using a DEEC, which performs the functions of the standard F100 engine controller. The DEEC provides both open-loop scheduling and closed-loop feedback control of fan airflow and engine pressure ratio. A more detailed description of the F100 EMD engine can be found in Myers and Burcham.[2] A diagram of the engine showing relevant instrumentation is shown in Fig. 1. The engine instrumentation is sampled at 20 Hz. Only the left engine was analyzed in this paper because it had research instrumentation at station 2.5 in addition to the standard set of operational instrumentation.

Parameter Estimation Process

The parameter estimation algorithm is a two-step process as shown in Fig. 2. The first step consists of a Kalman filter estimation of five deterioration parameters. These parameters are designed to model the off-nominal behavior of the engine during flight. They are the changes in efficiency of the low and high pressure turbine (DELPT and DEHPT), the changes in airflow in the fan and high pressure compressor (DWFAN and DWHPC), and a high pressure turbine area adder (AAHT). The second step is based on a simplified

steady-state model of the engine referred to in this paper as the compact engine model (CEM). In this step the control vector in the CEM is augmented by the deterioration parameters estimated in the first step. The deterioration parameters shift the model to more accurately reflect the actual operating condition of the engine. The CEM then produces estimates of the engine variables needed by the follow-on control laws. Flight measurements are used both to look up model data and as direct inputs for both the Kalman filter and the CEM. These two steps and their respective models are described in detail in the following sections.

Kalman Filter Implementation

The first step in the estimation algorithm is designed to identify the off-nominal characteristics of the engine when operating in a near steady-state condition. This is done by estimating five deterioration parameters with a Kalman filter.[7] These parameters are used to adjust the subsequent CEM to more closely match the measured flight data.

The state variable model (SVM) is used in the design and implementation of the Kalman estimator. It is a piecewise linear model representing the entire range of engine operation at 0.9 Mach, 30,000 ft altitude, standard day conditions. It consists of a state-space perturbation model and an associated table of steady-state trim values for all the engine variables in the model. The state-space perturbation model has the form

$$\Delta \dot{x} = [A]\Delta x + [B]\Delta u$$
$$\Delta y = [C]\Delta x + [D]\Delta u \qquad (1)$$

where

$$\Delta x = x - x_b$$
$$\Delta y = y - y_b$$
$$\Delta u = u - u_b$$

and associated Kalman filter formulation

$$\Delta \dot{\hat{x}} = [A]\Delta \hat{x} + [B]\Delta u + [K](\Delta y - \Delta \hat{y})$$
$$\Delta \hat{y} = [C]\Delta \hat{x} + [D]\Delta u$$

The state vector, x, control vector, u, and measurement vector, y, are defined as follows

$$x = \begin{matrix} N1 \\ N2 \\ TMT \\ DEHPT \\ DELPT \\ DWFAN \\ DWHPC \\ AAHT \end{matrix} \quad u = \begin{matrix} WF \\ AJEFF \\ CIVV \\ RCVV \\ HPX \\ BLD \end{matrix} \quad y = \begin{matrix} PT6 \\ PT4 \\ TT4.5 \\ N1 \\ N2 \end{matrix}$$

There are 49 sets of A, B, C, D, and K matrices corresponding to values of $PT4$ ranging from 23 to 260 lb/in^2 which accommodate the engine operating range for the flight envelope corrected to the Mach 0.90, 30,000 ft altitude reference condition. The SVM uses the set of matrices closest to the input value of $PT4$, with some intentional overlap of model ranges to avoid frequent model switching when operating at a $PT4$ close to halfway between models. The matrix elements were derived by perturbation and numerical differentiation of a large component-based nonlinear aerothermal simulation of the engine developed by the manufacturer. The last five states are intended to model engine deterioration. As such these parameters should be changing only very slowly and are modeled as locally constant, that is the last five rows of both the A and B matrices are zeros.

Figure 3 is a block diagram of the Kalman filter implementation. The Kalman gain matrix, K, was determined in advance assuming the system to be time invariant for near-steady-state engine operation. In determining the K matrix, the measurement noise intensity matrix was obtained from known engine statistics. The process noise intensity matrix was assumed to be the adjustable design parameter for the Kalman filter. The filter operates at 8 Hz. Details concerning the Kalman filter design can be found in Ref. 7.

The associated tables of steady-state trim values are scheduled as a bivariate function of $PT4$ and $PT6$. The tables are linearly interpolated over 7 values of $PT4$ and 40 values of $PT6$. The table, also derived from the full nonlinear simulation, consists of the predicted steady-state values of the x, y, and u vectors for a nominal undeteriorated engine over the entire flight envelope corrected to the design condition. These are the x_b, y_b, and u_b vectors in equation (1). The perturbation vectors input to the filter, Δu and Δy, are thus the

difference between flight condition corrected control and measurement vectors, and the trim predictions at each point in time. The trim predictions are computed for each sample of data input to the SVM using filtered values of $PT4$ and $PT6$, therefore the reference trim condition is constantly changing.

Values for the following measurements and control variables are taken directly from flight data: $N1$, $N2$, PB, $TT4.5$, $P6$, WF, CIVV, and RCVV. Additional engine and flight parameters are used indirectly by the Kalman filter algorithm for correcting the engine data and calculating other engine variables. These are $PT2$, $TT2$, $PS2$, P_{amb}, Mach, and PLA. The $PT4$ is calculated as a function of PB and $PT2$. The measured and calculated variables are corrected to the SVM design condition of Mach 0.90 and 30,000 ft altitude. Each engine variable has a correction factor that is a function of $PT2$ and $TT2$.

Three of the inputs to the Kalman filter, bleed air (BLD), horsepower extraction (HPX), and effective nozzle throat area ($AJEFF$) present special problems. The BLD and HPX are not measured. However analysis showed that at least the effect of bleed air was significant and needed to be explicitly accounted for in the model. The model matrices were linearized about an engine with no bleed or horse power extraction modeled. It was decided to explicitly include BLD and HPX as inputs to the model using the scheduled values of these parameters. The HPX is scheduled as a function of $N2$, and BLD is scheduled as a function of Mach and altitude. While these two inputs are known to vary from the nominal schedules, using the scheduled values is considered preferable to ignoring these effects. This approach allows the use of the same models for both engine test stand data with no bleed and actual flight data with bleed. Moreover the nominal schedules can be modified if flight test shows it to be warranted. A theoretically cleaner but perhaps less flexible approach would have been to derive the model matrices about an engine with the nominal bleed and horsepower extraction included and not have BLD or HPX as inputs. The nozzle throat area input was also a cause for concern. The measurement of the nozzle area is one of the poorer measurements on the system, in particular it is prone to measurement bias. Moreover the models were derived for subsonic operation without the afterburner. It was concluded that the model required an effective nozzle area rather than the actual measured nozzle area. Therefore the change in effective nozzle area input ($\Delta AJEFF$) is computed using the temperature and pressure measurements at station 6, the measured nozzle area, and the engine fuel flow.

Compact Engine Model

The second step in the estimation process is based on the CEM, which is a simplified steady-state simulation of the engine used to estimate the desired engine variables. The CEM consists of a linear steady-state perturbation model, steady-state trim tables, and follow-on nonlinear calculations. Figure 4 is a block diagram of the CEM.

The steady-state perturbation model (SSM) is a piecewise linear model that serves as the basis of the CEM. It is implemented as a steady-state perturbation model having the form

$$\Delta y = [F]\Delta u \qquad (2)$$

where

$$\Delta y = y - y_b$$

$$\Delta u = u - u_b$$

u and y represent the control input and measurement vectors respectively. They are defined to be

$$u = \begin{matrix} WF \\ PT6 \\ \text{CIVV} \\ \text{RCVV} \\ \text{HPX} \\ \text{BLD} \\ DEHPT \\ DELPT \\ DWHPC \\ DWFAN \\ DAAHT \end{matrix} \qquad y = \begin{matrix} N1 \\ N2 \\ AJ \\ PT2.5 \\ PT4 \\ TT2.5 \\ TT3 \\ TT4 \\ TT4.5 \\ TT6 \\ WCFAN \\ WCHPC \end{matrix}$$

This model was also derived by perturbation and numerical differentiation of the full nonlinear engine simulation at the Mach 0.90 and 30,000 ft altitude design condition. It was translated to the sea level static standard day reference condition using standard correction factors. The steady-state trim tables are analogous to those used with the SVM in the Kalman filter, providing the y_b and u_b vectors in equation (2). Both the SSM trim and the matrix models are scheduled as a bivariate function of $PT4$ and $PT6$ using linear interpolation between model points.

The SSM uses engine measurements for the following variables: WF, $PT6$, CIVV, and RCVV. As with the Kalman filter, additional flight parameters are used to calculate additional SSM inputs and correction factors. The HPX and BLD are again derived from schedules. The measured inputs are corrected to the SSM sea level static reference condition using correction factors that are a function of $PT2$ and $TT2$. The Kalman filter estimates of the deterioration parameters from the first step are input to the SSM calculation as the last five elements of the control vector. The F matrix and set of trim predictions are obtained for each sample of engine data as a function of $PT4$ and $PT6$, therefore the model and trim conditions may be constantly changing. The SSM provides estimates of the following variables at sea level static conditions: $N1$, $N2$, AJ, $PT2.5$, $PT4$, $TT2.5$, $TT3$, $TT4$, $TT4.5$, $TT6$, $WCFAN$, and $WCHPC$. These estimates are then recorrected to the original flight condition for comparison with flight values and for use in the subsequent nonlinear CEM calculations.

Following completion of the linear SSM calculation, the nonlinear CEM estimates are calculated at the original flight condition. These variables include $PT7$, $TT7$, FG, FNP, $DRAM$, $DNOZ$, AJ, SMF, and $SMHC$. The nonlinear calculations are based upon both measured engine variables and SSM estimates. They use a combination of analytical equations and empirically derived data tables. The $PT7$ and $TT7$ are calculated from the station 6 variables using afterburner heat addition and friction effects modified by afterburner efficiencies. Gross thrust is calculated as a function of the station 7 variables and overall airflow and fuel flow. The fan stall margin is a function of the fan pressure ratio $PT2.5/PT2$, $N1$, and CIVV position. The high compressor stall margin is calculated from a compressor disc pressure derived from $PT4$, the estimated $PT2.5$, and the RCVV position.

Maneuver Description

To evaluate how the Kalman filter would perform in a flight environment, flight data were obtained from the F-15 airplane. A maneuver was desired that would simulate a small change in engine operating efficiency at a near-steady-state flight condition. Defining such a maneuver was not trivial since normal aircraft maneuvers don't have much effect on engine operation except by changing the flight condition or introducing inlet distortion. There was also no way to introduce small perturbations to any of the standard engine controls. However, the pilot can selectively command the aircraft to get its bleed air only from either engine rather than both engines as is nominal. This would create changes in the bleed air flow and result in a small change in engine operation. A disadvantage of this potential maneuver was that the bleed air flow is not measured and thus is not known with much accuracy. At the time this flight experiment was being conducted, neither the SVM nor the SSM models had bleed or horsepower extraction as inputs. It was determined that switching the bleed air from one engine to the other was the best way to introduce a small unmodeled change to the engine operation to test the ability of PSC estimation algorithm to follow that change. The resulting change in engine operation was slightly larger than anticipated and early analysis of the results led to the reformulation of the models to include BLD flow and HPX as inputs to the model. The analysis in this paper uses the current models.

The maneuver flown consisted of flying at a stabilized flight condition with the bleed air coming from both engines for approximately 1 min, switching to get all the bleed air from the right engine for approximately 1 min, switching to get all the bleed air from the left engine for approximately 1 min, then returning to get the bleed air from both engines for 1 min. This was done at Mach 0.9, 30,000 ft altitude at left engine power lever angle (PLA) settings of 32°, 48°, and 83°. The PLA was varied to obtain a range in the $PT4$ and $PT6$ engine pressures. This is the model design condition so modeling errors should be at a minimum here.

The basic characteristics of this flight segment can be seen in the left engine response and control variables shown in Fig. 5. The BLD and HPX traces were synthesized from nominal schedules. Since BLD is not measured, the precise times of the bleed switches have been manually estimated based on pilot call-out during the flight and the secondary effects observed in other parameters. The bleed trace has been set to zero when the left engine bleed was switched off. The nominal schedules assume that the bleed air is coming equally from the two engines and follows the scheduled bleed curve as a function of Mach and altitude, however, the actual bleed flow from the two engines may differ substantially. When all the bleed airflow is coming from the left engine, the amount of increased airflow is indeterminate. No attempt has been made to model this increase.

Kalman Filter Results

This section presents the Kalman filter estimates of the deterioration parameters. The deterioration parameters are intermediate values in the estimation process and have no standards for comparison. The engineering meaning of these parameters is somewhat nebulous because in addition to actual changes in engine efficiency, they pick up Reynolds effects which are not accounted for in the model, sensor biases, and errors in the steady-state trim tables. Their primary function in this estimation algorithm is to shift the CEM to more closely match flight data. The only concrete way to evaluate the deterioration parameters is to observe their effects on the CEM parameter estimates. This will be done in the section on the performance of the CEM. They will however, be presented here with some primarily qualitative discussion. The flight segment analyzed contains two large PLA changes (Fig. 5(a)); these changes cause substantial model changes and large engine transients. The algorithm was designed for near-steady-state operation and as such, the filter results during the PLA transient are in transition and should be ignored.

The data were evaluated with two bleed models. In the first, the nominal bleed schedule was used throughout the flight segments, including when the bleed flow from that engine had been cut off by the pilot. This case represents an unmodeled disturbance. The change in bleed flow from the engine can only be detected by the Kalman filter indirectly through changes in the other variables. Since bleed is input as being constant, the changes in engine operation caused by actual changes in the bleed should appear as a change in the engine operating efficiency. In the second case, the nominal bleed flow model was overridden with a zero input when the bleed was known to be turned off. Therefore in this case the Kalman filter model knows about the change in bleed airflow and should accommodate expected changes in other variables without changing the deterioration parameters. Recall BLD is not a measured variable and the nominal bleed schedule is only a reasonable guess, and thus is a probable source of modeling error that will show up as changes in the deterioration parameters. Moreover, the maneuver also had approximately a 1-min segment when all the bleed air was being pulled from the left engine. As such the bleed air taken from the engine was probably higher than nominal during that minute; however, as reasonable numbers for how much higher are not available the nominal bleed level was used here.

The control inputs to the Kalman filter are shown in Fig. 6. These inputs are the difference between the measured control values and the predicted trim values of those controls. An example of this process is shown in Fig. 7 for fuel flow, the bottom plot shows the actual measured fuel flow plotted with the trim values. The resulting difference, ΔWF, is shown in the top plot. Note that some of the more pronounced changes in ΔWF are caused by the measurement and the trim value moving in opposite directions, this is particularly evident when the bleed was switched off at about 720 sec. The trim table values for BLD and HPX are zero. The five measurement inputs are shown in Fig. 8. Again these are the differences between the measured values and the trim values scheduled as functions of $PT4$ and $PT6$. The trim lookups are done with filtered values of $PT4$ and $PT6$ so the $\Delta PT4$ and $\Delta PT6$ traces are simply the difference between the unfiltered and the filtered values. The residuals for these five variables are shown in Fig. 9, indicating that at least steady-state, good matches were obtained.

The deterioration parameters for the Mach 0.9 and 30,000-ft altitude flight segment are shown in Fig. 10. Shown are the values for the deterioration parameters both with a nominal bleed assumed throughout and with the bleed input set to zero when the bleed was switched off. The bleed maneuver has a pronounced effect on the five deterioration parameters, particularly at the lower PLA settings. The Kalman filter seems to handle the resulting transient well. The low turbine deterioration parameter tends to increase over the flight segment, while the high turbine deterioration parameter decreases. This effect may be more of an indication of difficulty in separately identifying the two parameters than a real change in the efficiency of either turbine. Studies have shown that a bias in the $TT4.5$ sensor can have this effect and there is some reason to believe that the flight data does have a bias exceeding the instrumentation specification.

The engine deterioration parameters are modeled as locally constant, as was mentioned in the discussion of the Kalman filter implementation and as is more extensively discussed in Ref. 7. These parameters are picking up relatively constant differences between the measured engine variables and the predicted trim values for those variables for a nominal engine. Thus

the parameters should model how far the steady-state engine deviates from the theoretical nominal engine. One obvious problem with this formulation is that instrumentation biases will appear as the same type of constant offset from the trim values and thus will end up being reflected in the deterioration parameters. The current set of control system sensors is insufficient to separately identify the engine deterioration parameters and sensor biases.[7] This data was obtained from an old engine nearing an overhaul; however, the control system sensors are representative of fleet type engines. It was anticipated that both deterioration and sensor biases would exist on the data being analyzed. This situation is probably typical of real engines in the field and is the reason an engine adaptive algorithm is desired. Nonetheless it clearly represents a challenging first test case.

Compact Engine Model Results

There are three means by which the CEM results can be assessed. First, five of the CEM estimates are also input measurements to the Kalman filter. Since this estimation process makes no attempt at estimating measurement biases, these estimates should match the measurements closely. However, because these are input measurements to the estimation process, a good fit for these variables does little to ensure that the other estimates are equally as good. Second, for two of the CEM estimates there are truly independent checks available. This engine has been instrumented with pressure and temperature sensors at engine station 2.5 that are not generally available on the F100 engine and thus were not used in the estimation algorithm. Results will be compared to two temperature sensors and to the average of five pressure sensors located at station 2.5. The station 2.5 engine pressure and temperature estimates are inputs to both of the nonlinear stall margin calculations and therefore are also key to the quality of the stall margin estimates. A weaker independent check for the fan airflow estimate also exists. The DEEC logic has a simple estimate of the fan airflow that is used in the DEEC control laws. This estimate is dependent on a nominal engine operating on the nominal operating line. However, previous flight tests of this engine with extra instrumentation have indicated that the current airflow estimate is accurate. It is the opinion of the engine manufacturers that the CEM estimated fan airflow should be better than the DEEC engine estimate, however, based on previous flight-test experience the DEEC estimate does provide another reasonable independent check of the CEM estimates. Third, it is interesting to observe how sensitive the estimates are to the bleed airflow model and to the deterioration estimates. A high degree of sensitivity to either the bleed airflow model or the deterioration estimates would definitely be cause for concern.

The CEM estimates of the five measured inputs ($N1$, $N2$, $PT4$, $TT4.5$, and AJ) track the measurements extremely well at all three PLA settings (Fig. 11) with the traces for the measured and estimated data being indistinguishable for all but AJ on the scales shown. For the independent sensors at engine station 2.5, Fig. 12, the agreement between the estimates and the flight measured data is poorer. The two temperature probes disagree by approximately 10° at the 32°-PLA setting, and are in good agreement with one another at the 48°- and 83°-PLA settings. The CEM $TT2.5$ estimate is approximately 15° to 25° higher than either probe throughout. The CEM $PT2.5$ estimate gives excellent agreement with the average measured $PT2.5$ for PLA settings of 32° and 48° but at a PLA setting of 83°, the estimate is approximately 0.5 lb/in^2 low. The CEM estimated fan airflow also agrees with the engine airflow estimate at the 32°- and 48°-PLA settings but is about 5 lb/sec high at the 83°-PLA setting. The comparison of these three parameters is replotted in Fig. 13 for the 83°-PLA setting. The difference for all three parameters is primarily a constant offset throughout the segment, however the traces do not really track each other closely even if the offset is removed.

A representative example of the estimator's sensitivity to bleed modeling is shown in Fig. 14. Eight of the estimated parameters at Mach 0.90, 30,000 ft with a PLA of 48° are shown. Each plot shows both the estimate using the nominal bleed model throughout and the estimate obtained when the nominal bleed model was zeroed when the bleed from the left engine was off. Additionally, the flight data is plotted when available. From these plots one can determine the sensitivity of the CEM to a bleed modeling error of 100 percent of the nominal bleed and therefore determine whether using the nominal bleed model is acceptable for the intended application. The most interesting result here is seen in the $PT2.5$ traces. The flight data clearly shows an increase in the pressure when the bleed flow is turned off (time = 40 sec). When the bleed is erroneously assumed to be at the nominal level throughout, a similar small rise is seen in the estimated $PT2.5$

trace. However, when the bleed model is zeroed when the bleed is turned off, the $PT2.5$ estimate remains fairly constant and does not predict the pressure change at station 2.5. While the effect is small, this discrepancy indicates a modeling problem in the estimation process. In contrast, for both $TT2.5$ and fan airflow, modeling the bleed off does make the estimate match the flight data more closely. While the effects of modeling the bleed incorrectly are noticeable in many of the key unmeasured estimates, the sensitivity to this error is not excessive and the estimates probably would still be acceptable for most applications. Since the nominal bleed schedule is only a coarse estimate for the actual bleed airflow these results are reassuring. However, the cumulative effect of multiple errors of this magnitude would be a problem.

The estimated deterioration parameters contribute significantly to the values of the CEM output parameters. Figure 15 shows overplots of the flight measured data and the CEM estimates with and without the Kalman filter derived deterioration parameters for the five measured inputs for the 32°-PLA condition. The bleed model used is identical for both estimates and has the nominal bleed model zeroed when the bleed was switched off. As was previously noted, (Fig. 11) the agreement between the measured data and the estimates from the full algorithm is excellent for these parameters. However, from the overplots (Fig. 15) it is also apparent that the high quality of the fit is dependent on the estimated deterioration parameters. The estimates obtained without using the deterioration parameters to correct the CEM to the flight data are poor, and probably would not be acceptable for many applications. Thus it appears that the engine adaptive features of the estimation algorithm provided by the Kalman filter are necessary. However, since the Kalman filter used these five measurements to obtain the deterioration estimates, agreement of these variables is not sufficient to guarantee similar accuracy in the other estimated engine variables. The hope is that the estimates of the unmeasured variables will be similarly improved by matching the responses of these major engine variables.

Comparisons of the estimates with the three independent flight data parameters are shown in Fig. 16. The estimates of $PT2.5$ and $WCFAN$ match the flight data substantially better, and the $TT2.5$ estimate is somewhat improved when the deterioration estimates are used. Similar results for these three parameters were also obtained at a PLA of 48°. However, at the 83°-PLA condition shown in Fig. 17, the estimates for both $PT2.5$ and $WCFAN$ move away from the flight data when the deterioration estimates are used, while the $TT2.5$ estimate is again somewhat improved. The amount that the $PT2.5$ and $WCFAN$ estimates moved away from the flight data is small enough not to be of serious concern in itself, however, it does raise the question of whether the deterioration parameters will generally improve the estimates of the unmeasured variables.

For the other CEM estimates no standards of comparison are available. The comparisons for three of these parameters (the SMF, $SMHC$, and FNP) are shown in Fig. 18 for the 32°-PLA case and Fig. 19 for the 83°-PLA case. Note that in the 32°-PLA case the CEM predicts the high compressor stall margin to be up to 15 percent higher and the fan stall margin up to 5 percent higher with the deterioration parameters. At the 83°-PLA condition (intermediate power) there is little change in the high compressor stall margin and a steady 5-percent increase in the fan stall margin. Caution should be used in trading this extra computed stall margin for performance gains. The thrust calculation appears to be far less sensitive to the deterioration parameter estimates. There is a negligible change in the thrust estimate at the 32°-PLA setting (Fig. 17) and only a small change at the 83°-PLA setting (Fig. 18).

Concluding Remarks

Based on the theoretical formulation and the limited evaluation using flight data, it appears that the performance seeking control (PSC) estimation algorithm can provide reasonable estimates of an extended set of engine variables needed for advanced propulsion control law development. However, the conclusions drawn from this investigation are limited because of a lack of high quality independent flight measurements of many of the variables being estimated. This will also be a problem in the performance seeking control (PSC) flight-test evaluation program. Additional sensors or independently derived estimates of many of the extended variables are needed to firmly establish the validity of the estimation algorithm.

The adaptive nature of the PSC algorithm is primarily provided by the Kalman filter determined deterioration parameters. A comparison of the estimates of the measured variables with and without the deterioration parameters indicates that the nominal engine model is not adequate, and off-nominal performance must be accounted for in an engine estimation algorithm. However, the success of the deterioration parameters in matching the compact engine model (CEM) to flight data for the measured variables cannot be assumed to extend to the unmeasured variables. One case is presented in which the deterioration parameters move the CEM estimate further away from the flight data. The stall margin calculations seem to be particularly sensitive to the deterioration parameter estimates. In the cases shown there was a significant increase in the two stall margin estimates caused by using the deterioration parameters. Since the change is in an unconservative direction, it is not clear how much of the stall margin increase should be taken advantage of, until further confidence in these estimates has been established. Because of the model structure and limited input measurements available, it is not possible to separate actual engine deterioration from sensor biases, Reynolds effects, and other unmodeled phenomena or modeling errors.

References

[1] Tich, E.J., Shaw, P.D., Berg, D.F., Adhibatla, S., Swan, J.A., and Skira, C.A., "Performance Seeking Control for Cruise Optimization in Fighter Aircraft," AIAA-87-1929, June 1987.

[2] Burcham, F.W., Jr., Myers, L.P., and Walsh, K.R., *Flight Evaluation Results for a Digital Electronic Engine Control in an F-15 Airplane*, NASA TM-84918, 1983.

[3] Myers, L.P., and Burcham, F.W., Jr., *Preliminary Flight Test Results of the F100 EMD Engine in an F-15 Airplane*, NASA TM-85902, 1984.

[4] Baer-Riedhart, Jennifer L., and Landy, Robert J., *Highly Integrated Digital Electronic Control-Digital Flight Control, Aircraft Model Identification and Adaptive Engine Control*, NASA TM-86793, 1987.

[5] Proceedings of a minisymposium held at NASA Ames Research Center Dryden Flight Research Facility, Edwards, California May 25–26, 1983, *Digital Electronic Engine Control (DEEC) Flight Evaluation in an F-15 Airplane*, NASA CP-2298.

[6] Proceedings of a conference held at NASA Ames Research Center, Dryden Flight Research Facility, Edwards, California, March 11–12, 1987. *Highly Integrated Digital Electronic Control Symposium*, NASA CP-3024.

[7] Luppold, R.H., Gallops, G., Kerr, L., and Roman, J.R., "Estimating In-Flight Engine Performance Variations Using Kalman Filter Concepts," AIAA-89-2584, July 1989.

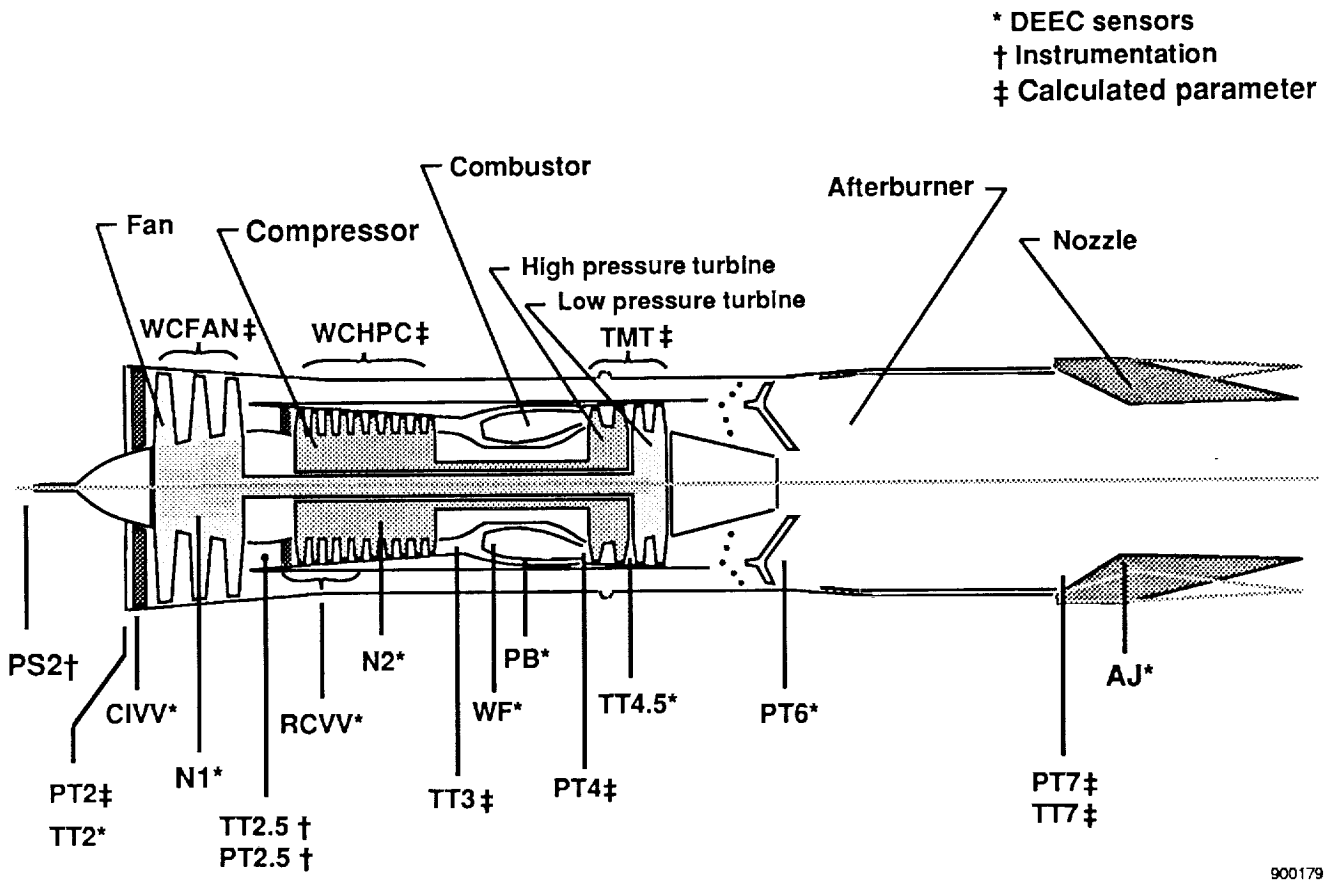

Fig. 1 F100 engine and sensor locations.

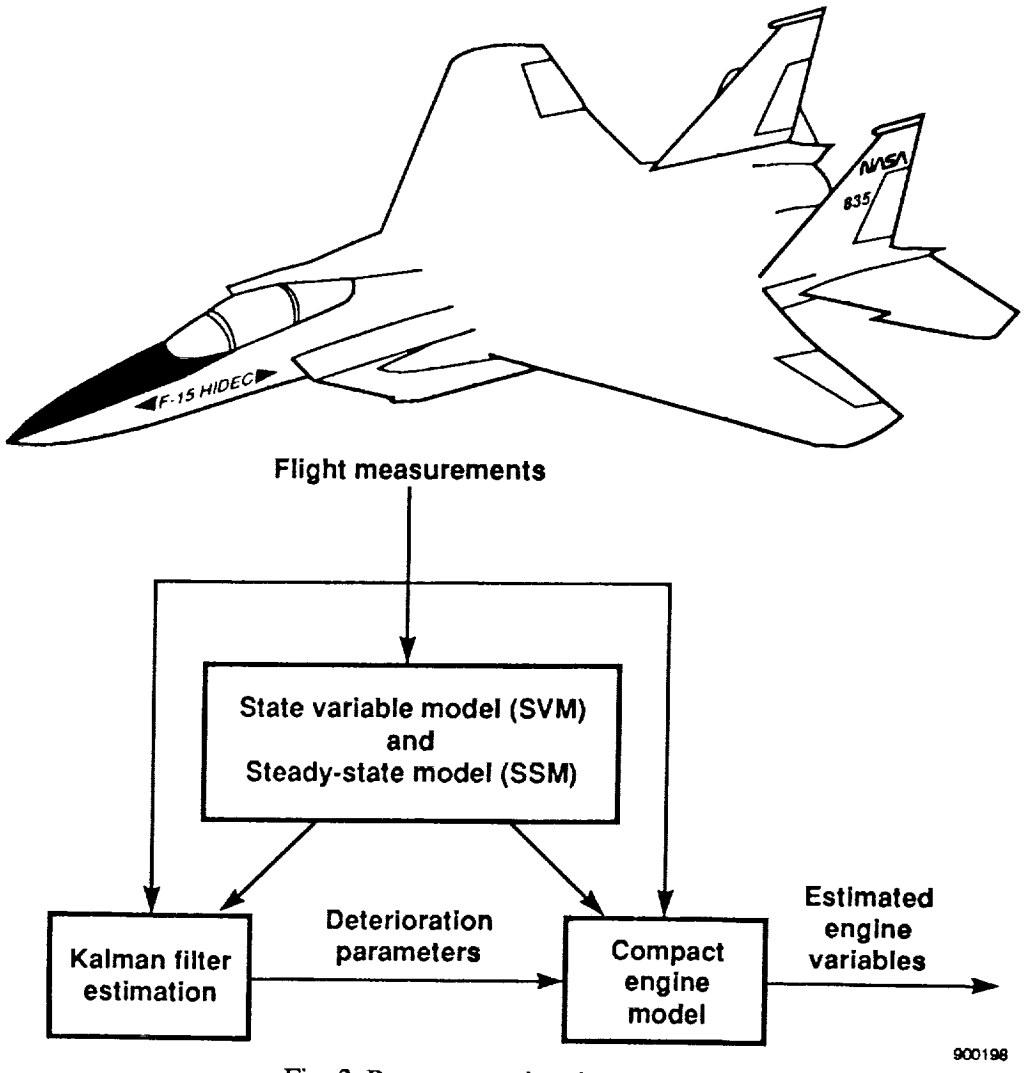

Fig. 2 Parameter estimation process.

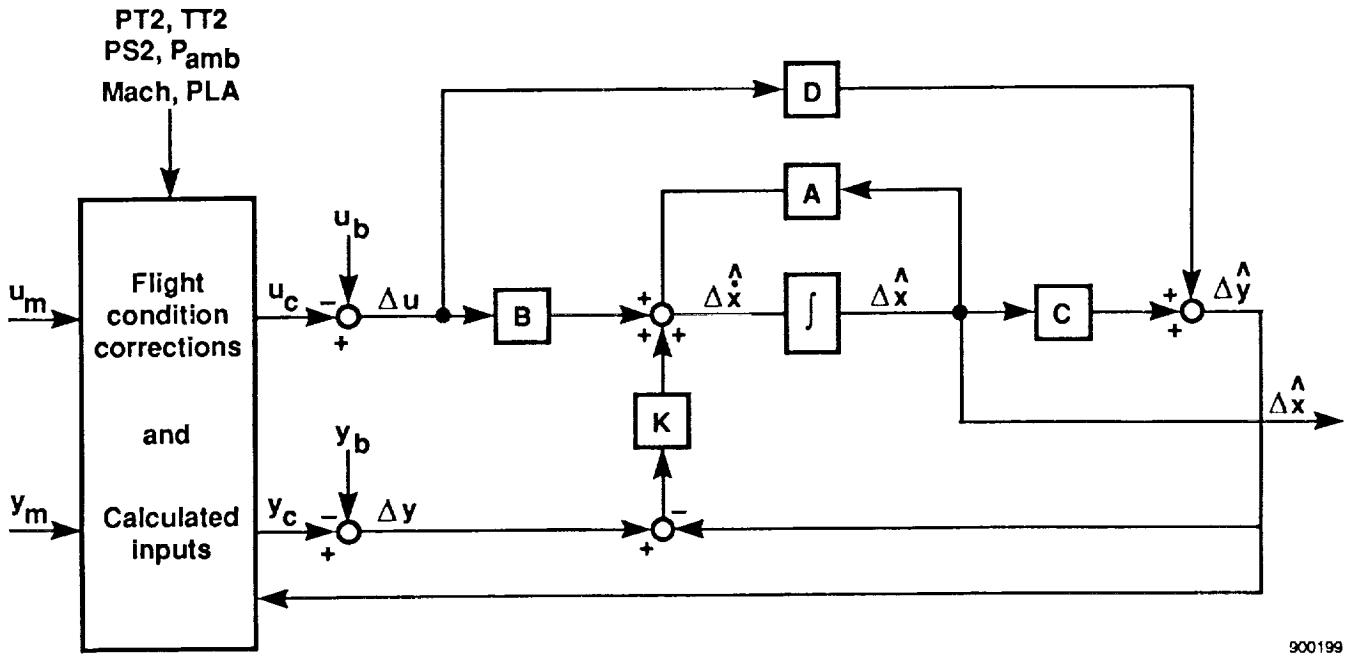

Fig. 3 Extended Kalman filter structure.

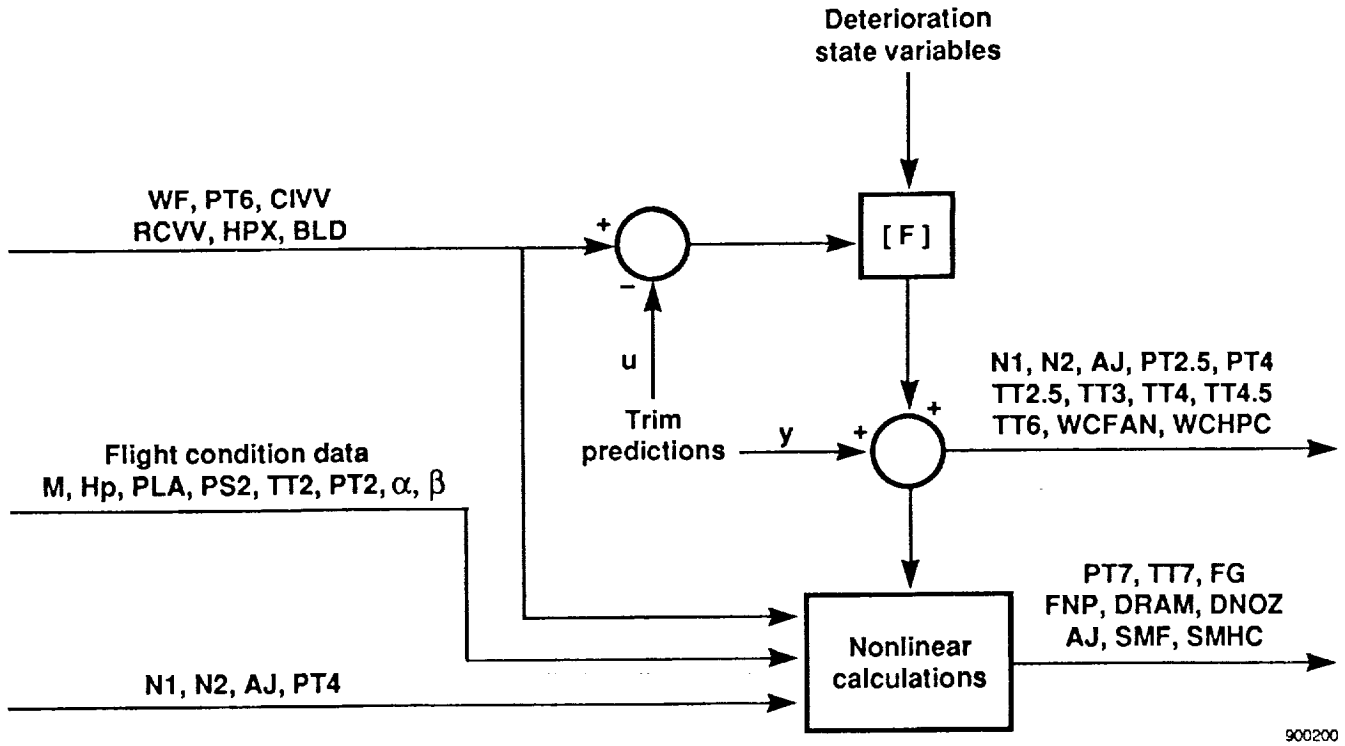

Fig. 4 Compact engine model.

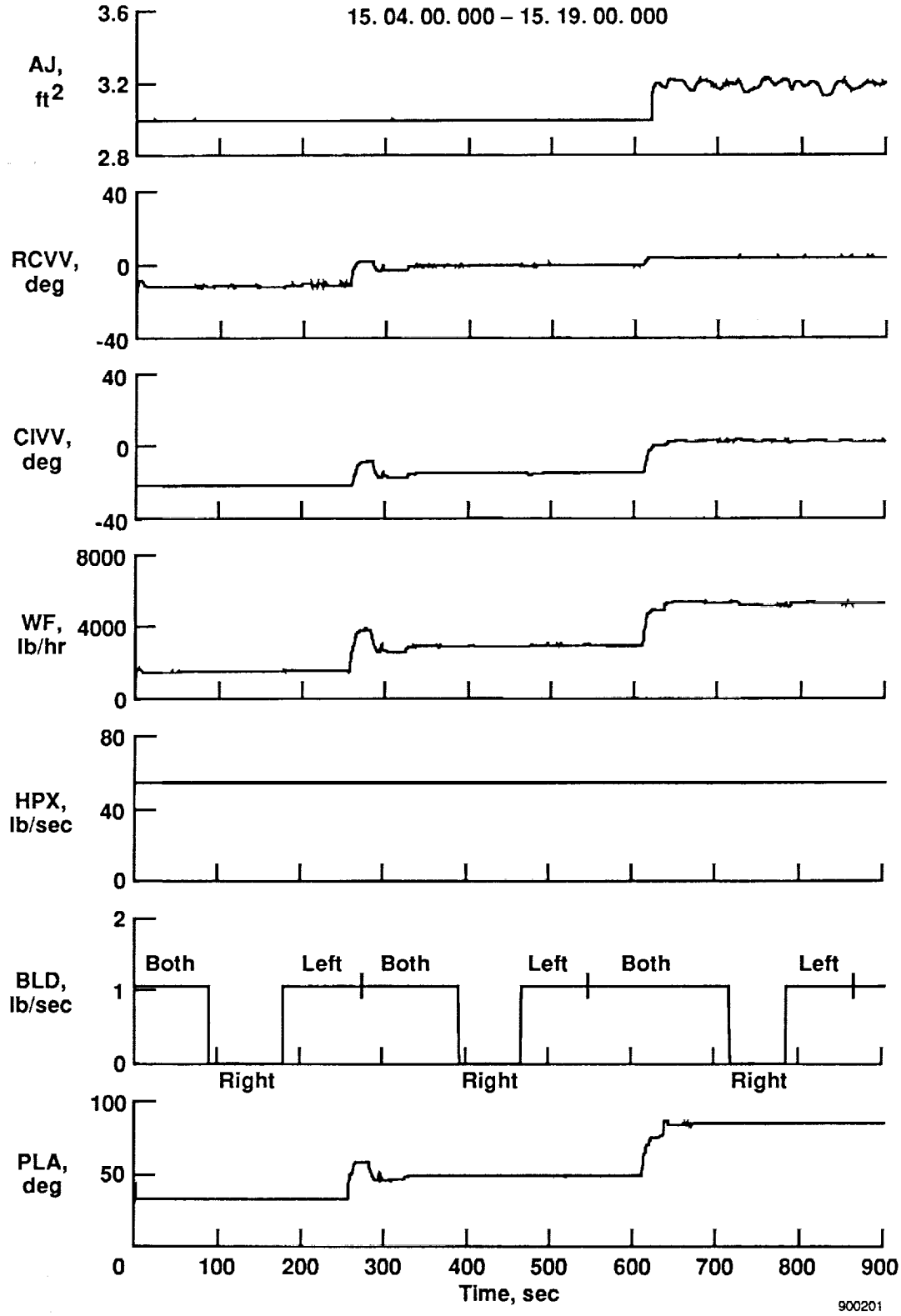

(a) Engine control inputs.

Fig. 5 Bleed change maneuver; Mach 0.90 and 30,000-ft altitude.

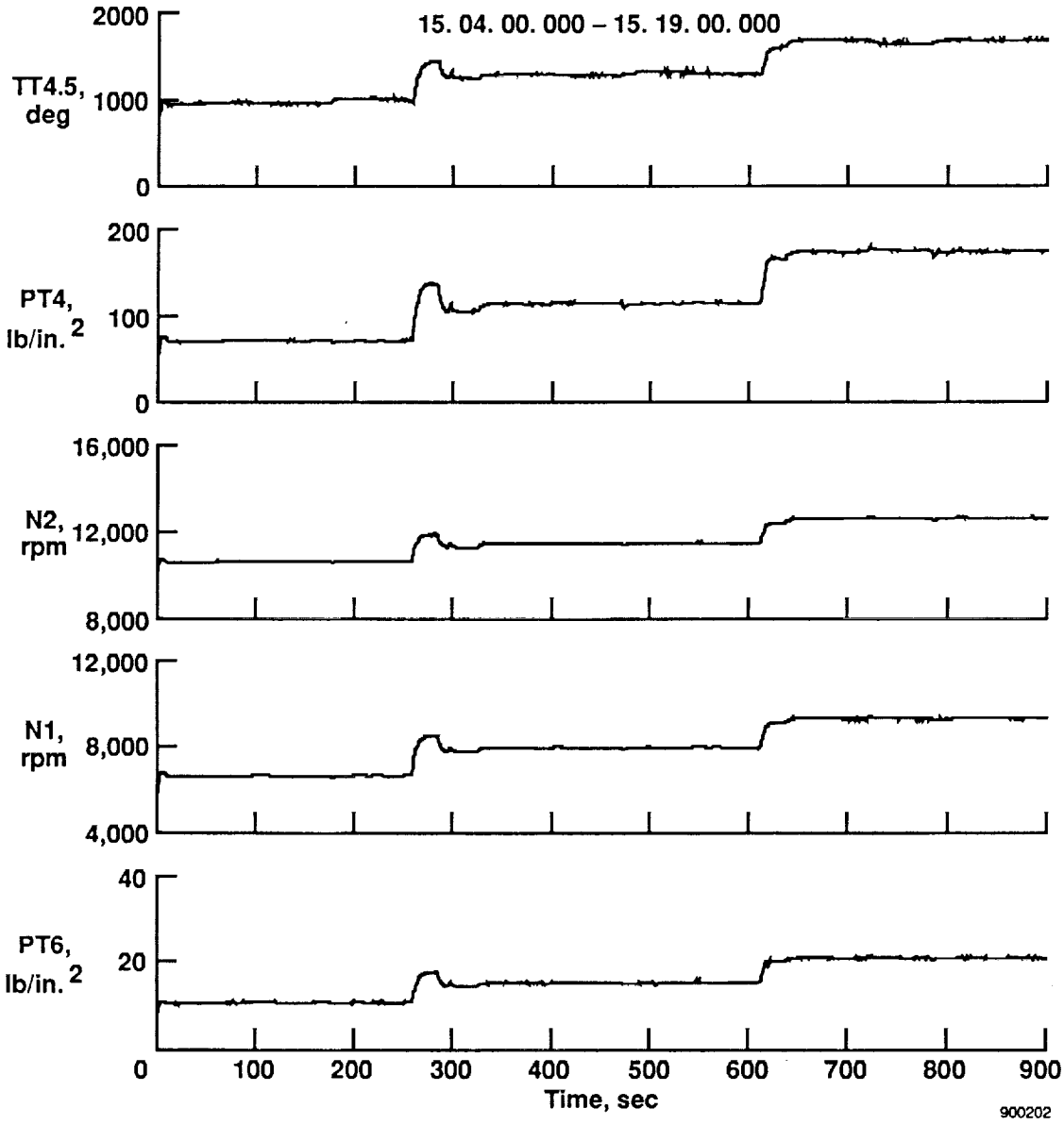

(b) Engine response characteristics.

Fig. 5 Concluded.

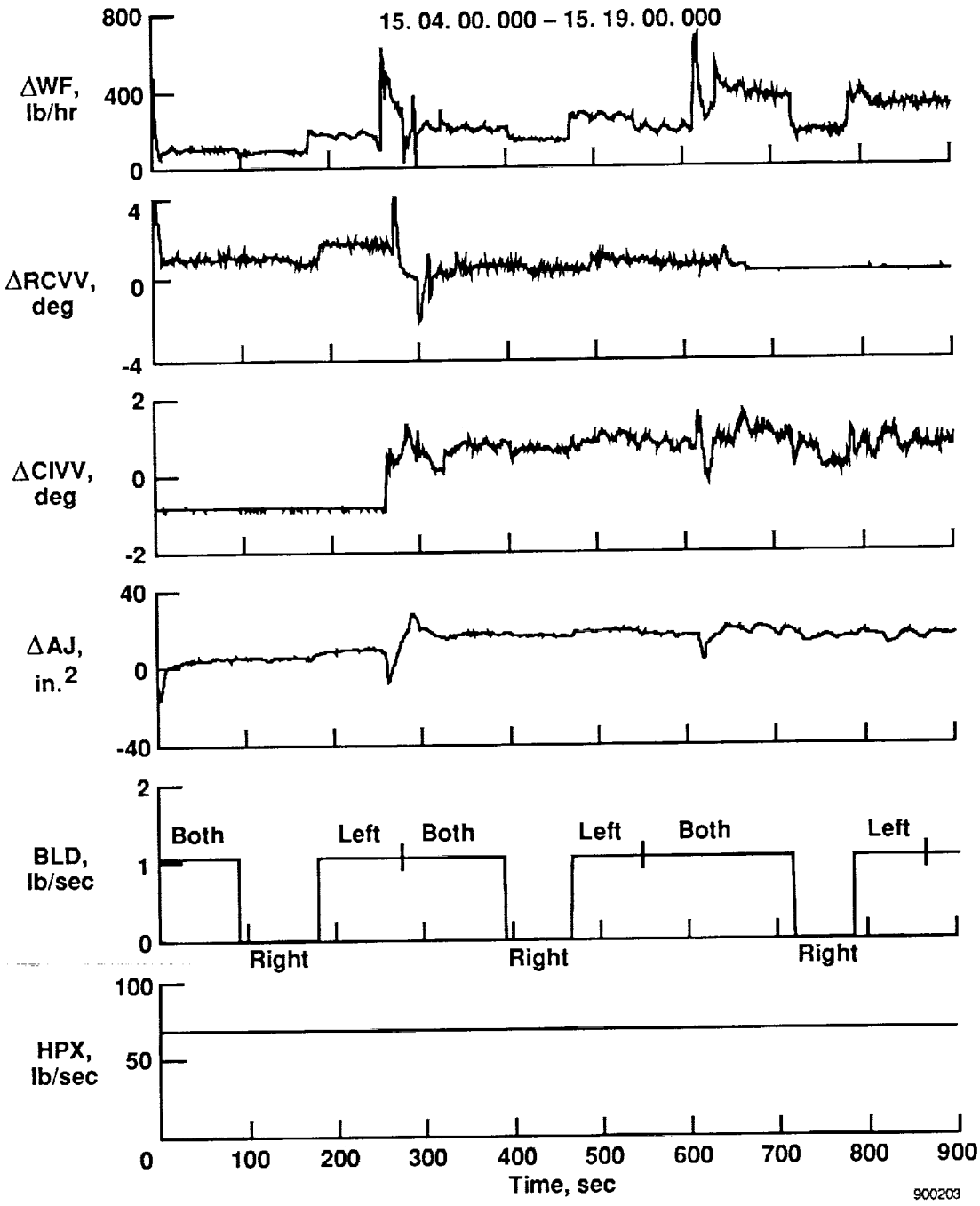

Fig. 6 Perturbation control inputs to the Kalman filter.

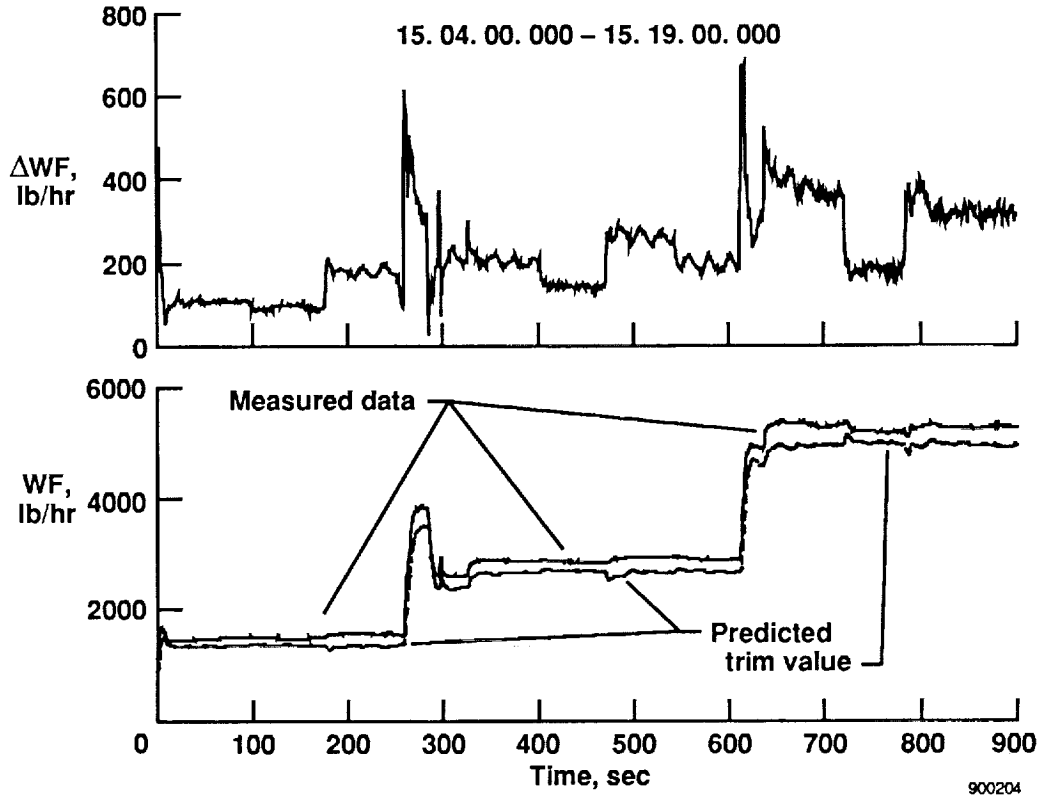

Fig. 7 Relationship of flight data and predicted trim data to the Kalman filter perturbation control input for fuel flow.

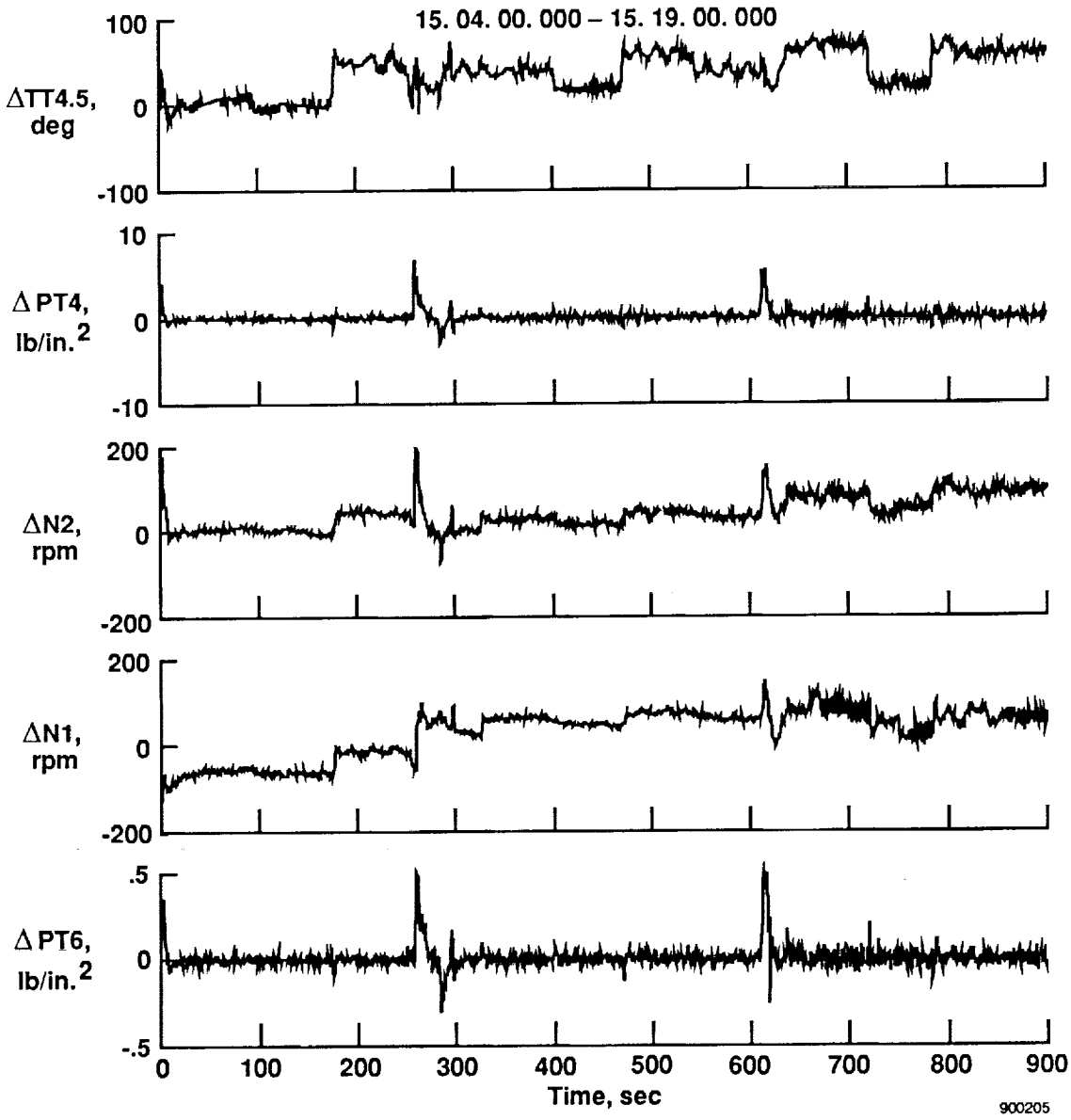

Fig. 8 Perturbation response inputs to the Kalman filter.

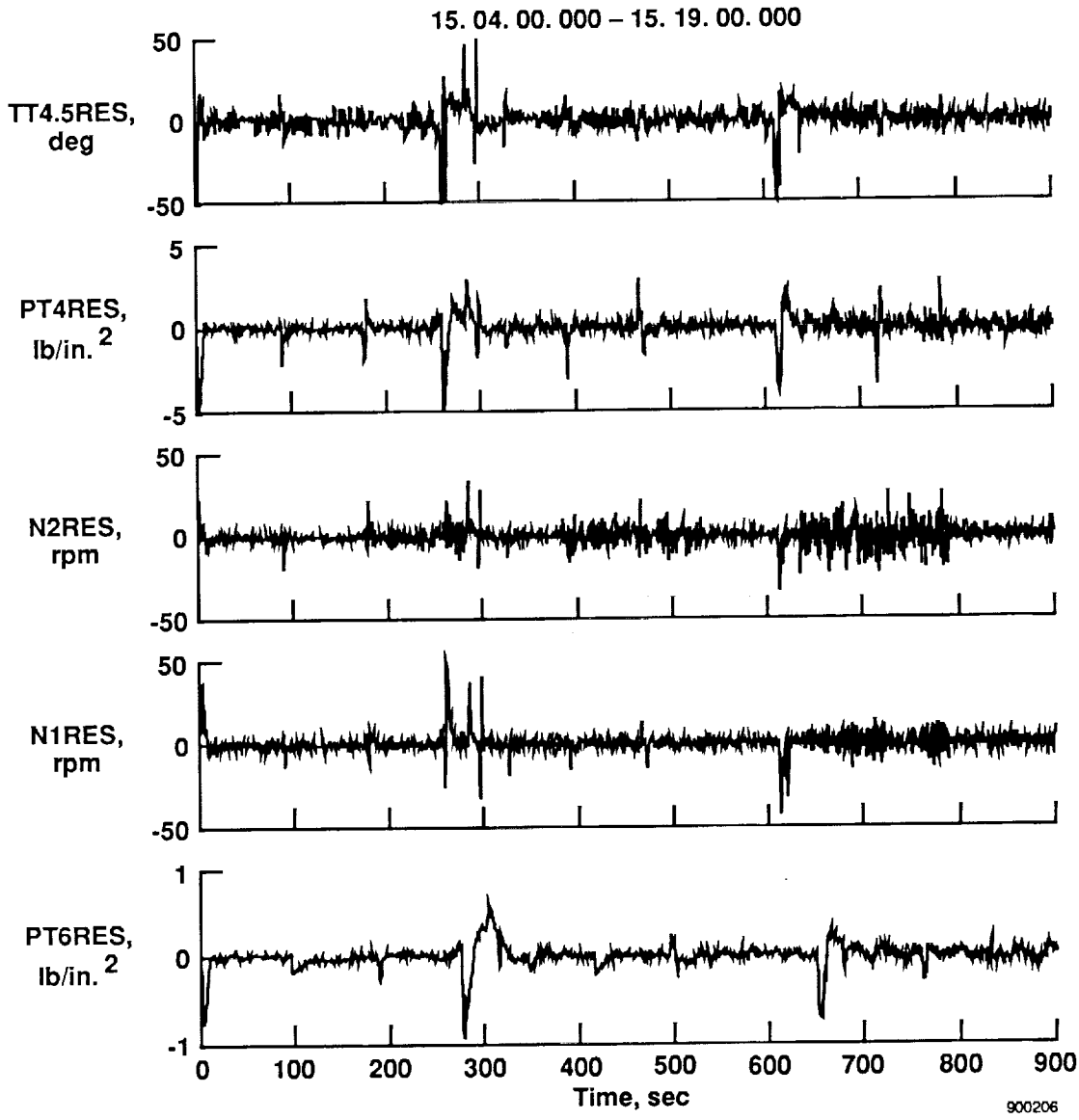

Fig. 9 Kalman filter output residuals.

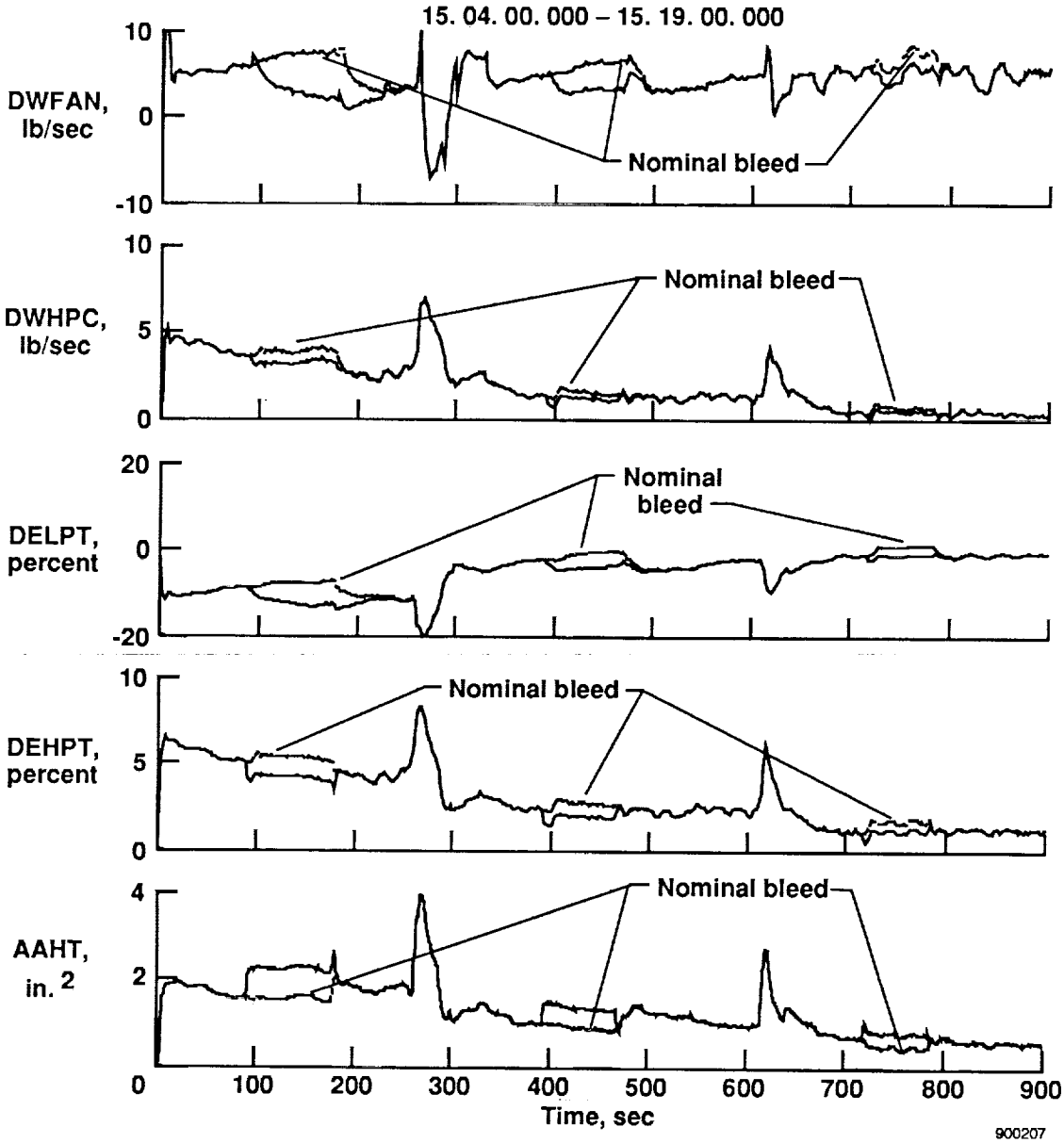

Fig. 10 Kalman filter estimate of state deterioration parameters.

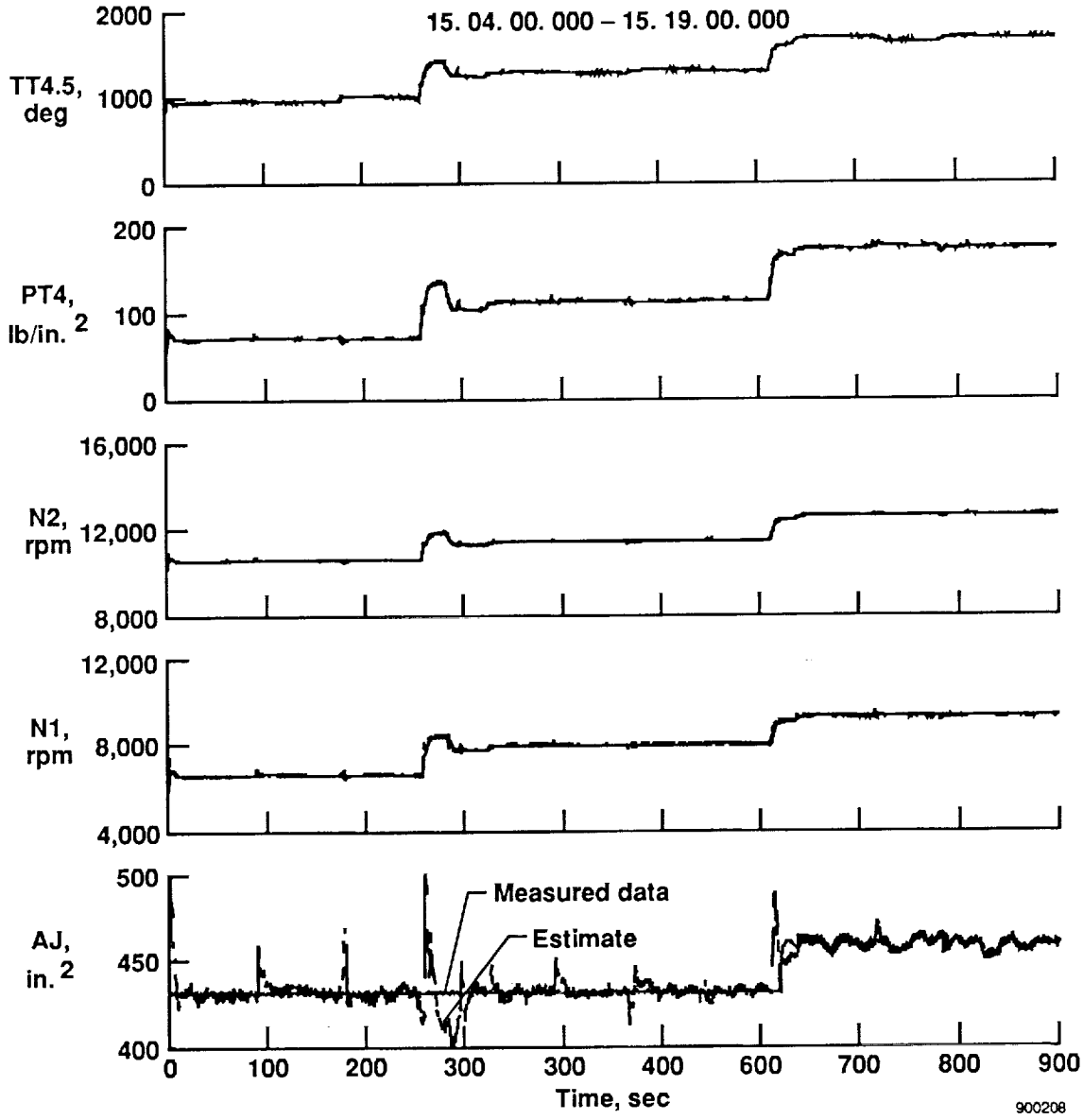

Fig. 11 Comparison of CEM estimates and flight data measurements.

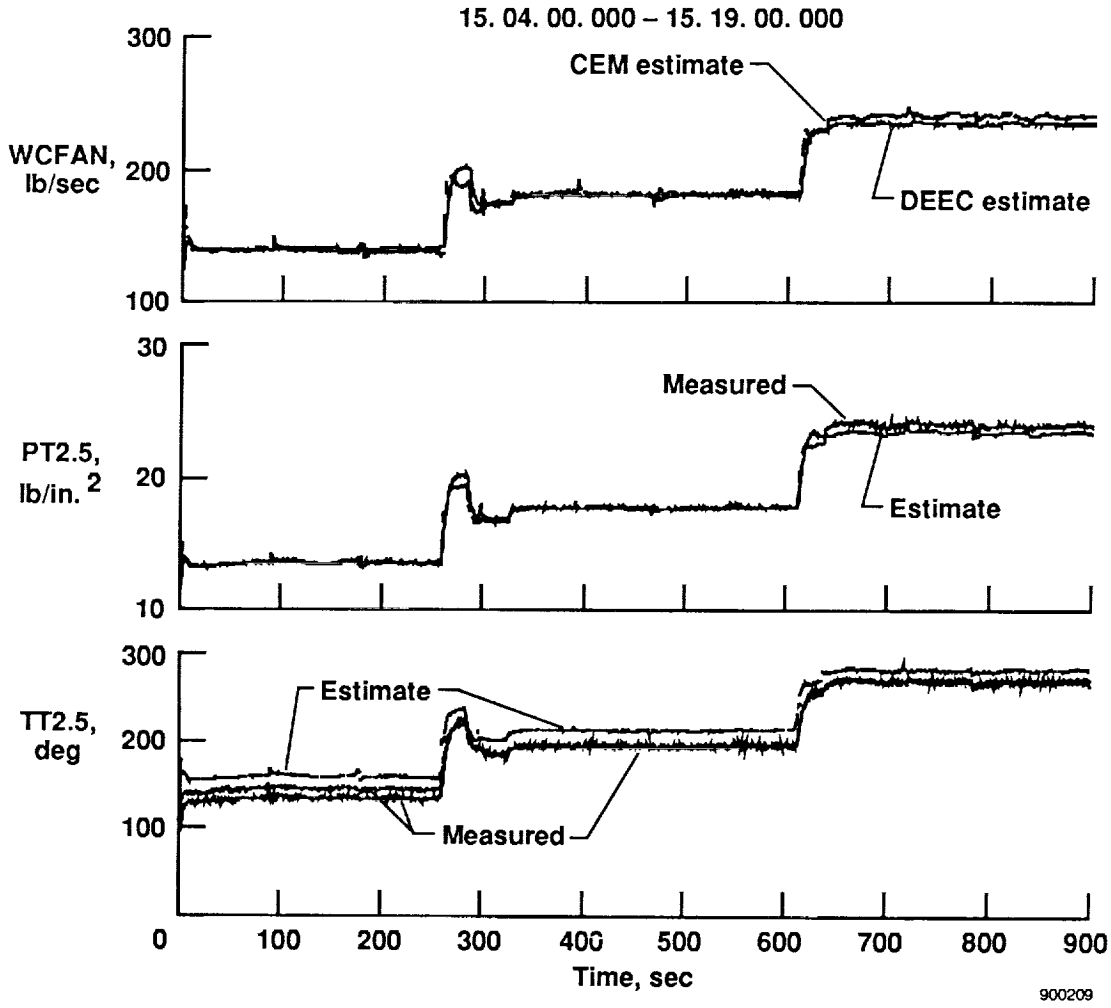

Fig. 12 Comparison of CEM estimates and flight data measurements for variables not used in the Kalman filter estimator.

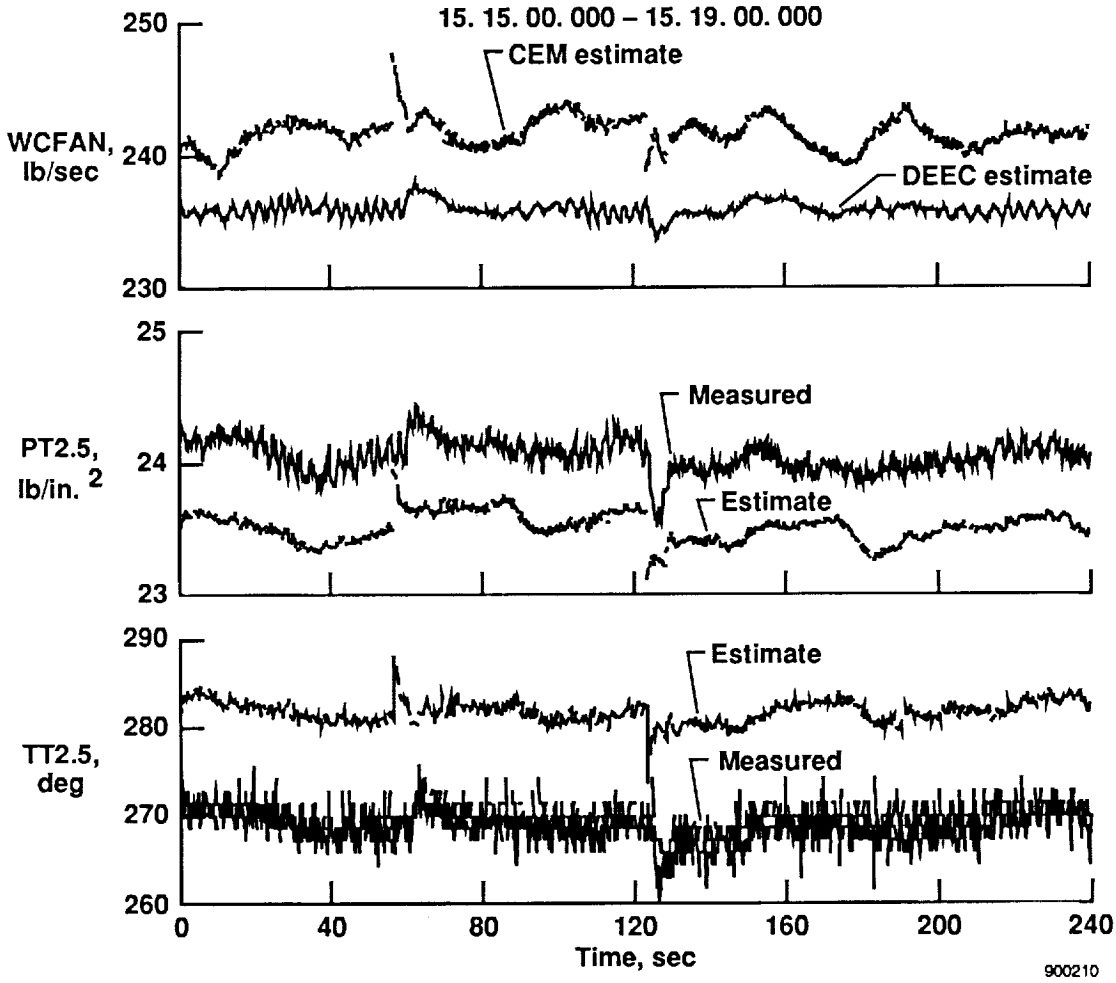

Fig. 13 Comparison of CEM estimates and flight data for PLA = 83°.

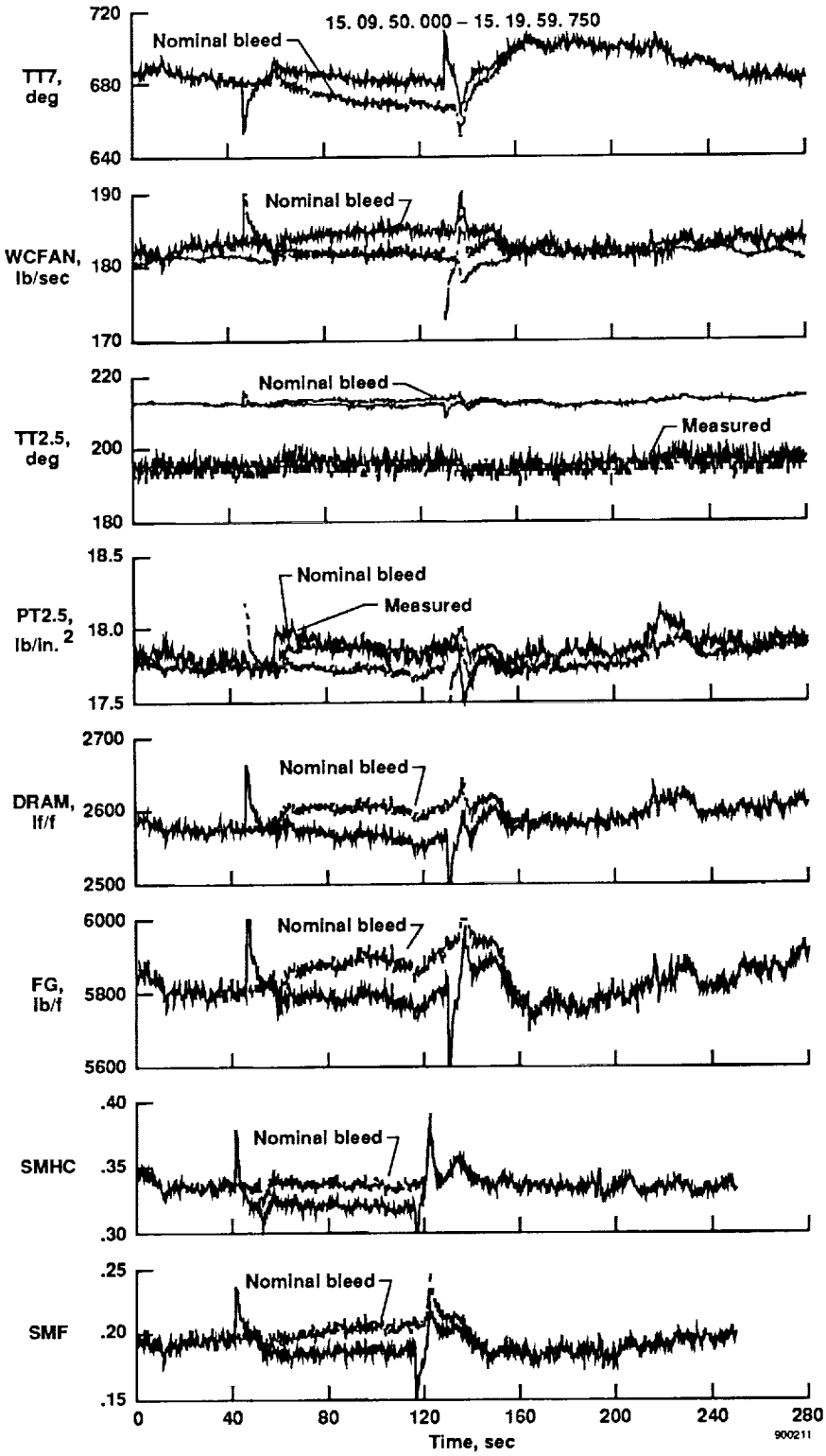

Fig. 14 Sensitivity of CEM estimates to bleed airflow modeling for PLA = 48°.

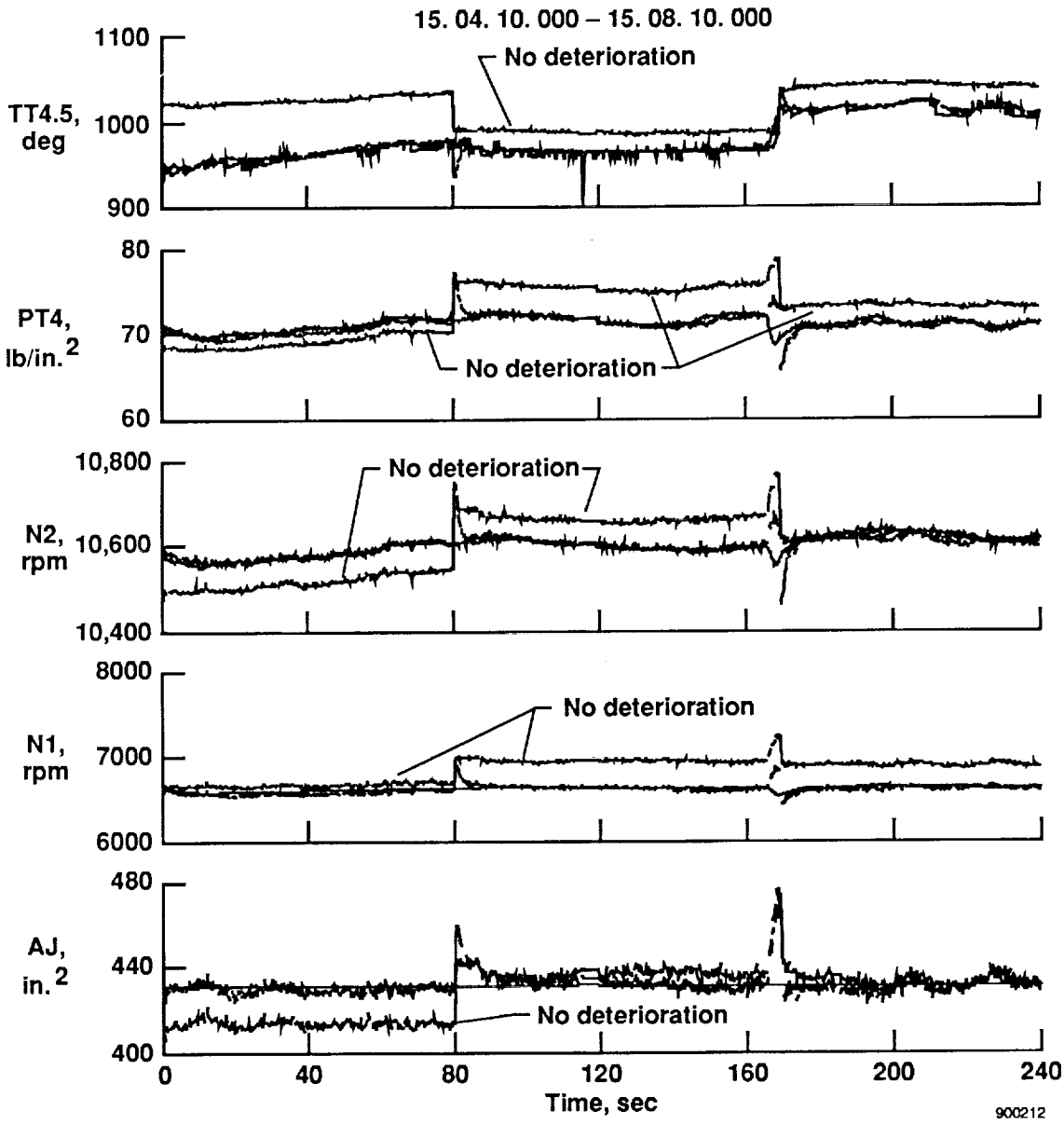

Fig. 15 Comparison of CEM estimates (with and without accounting for deterioration with flight measurements for PLA = 32°.

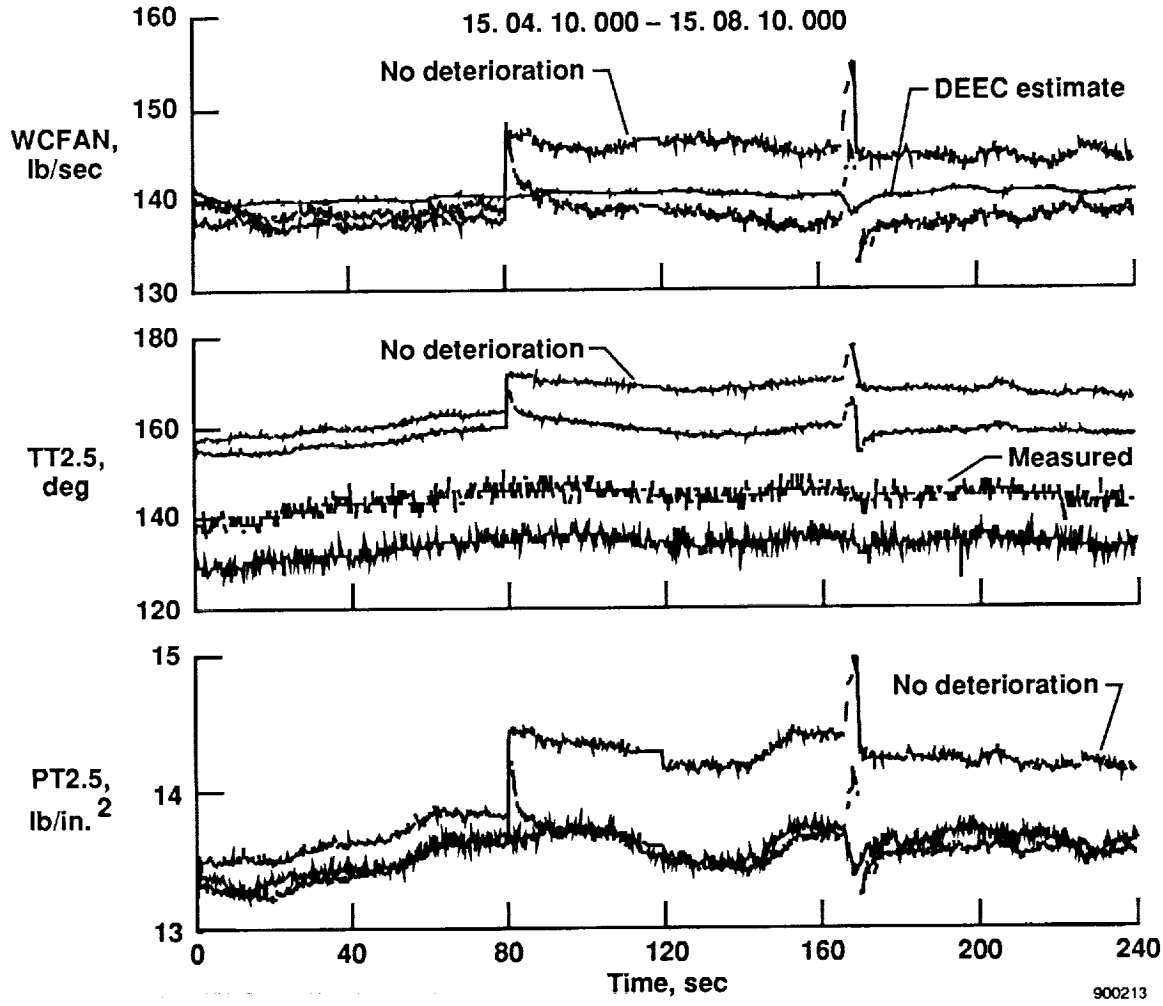

Fig. 16 Comparison of CEM estimates (with and without accounting for deterioration) with flight measurements not used in the Kalman filter estimator for PLA = 32°.

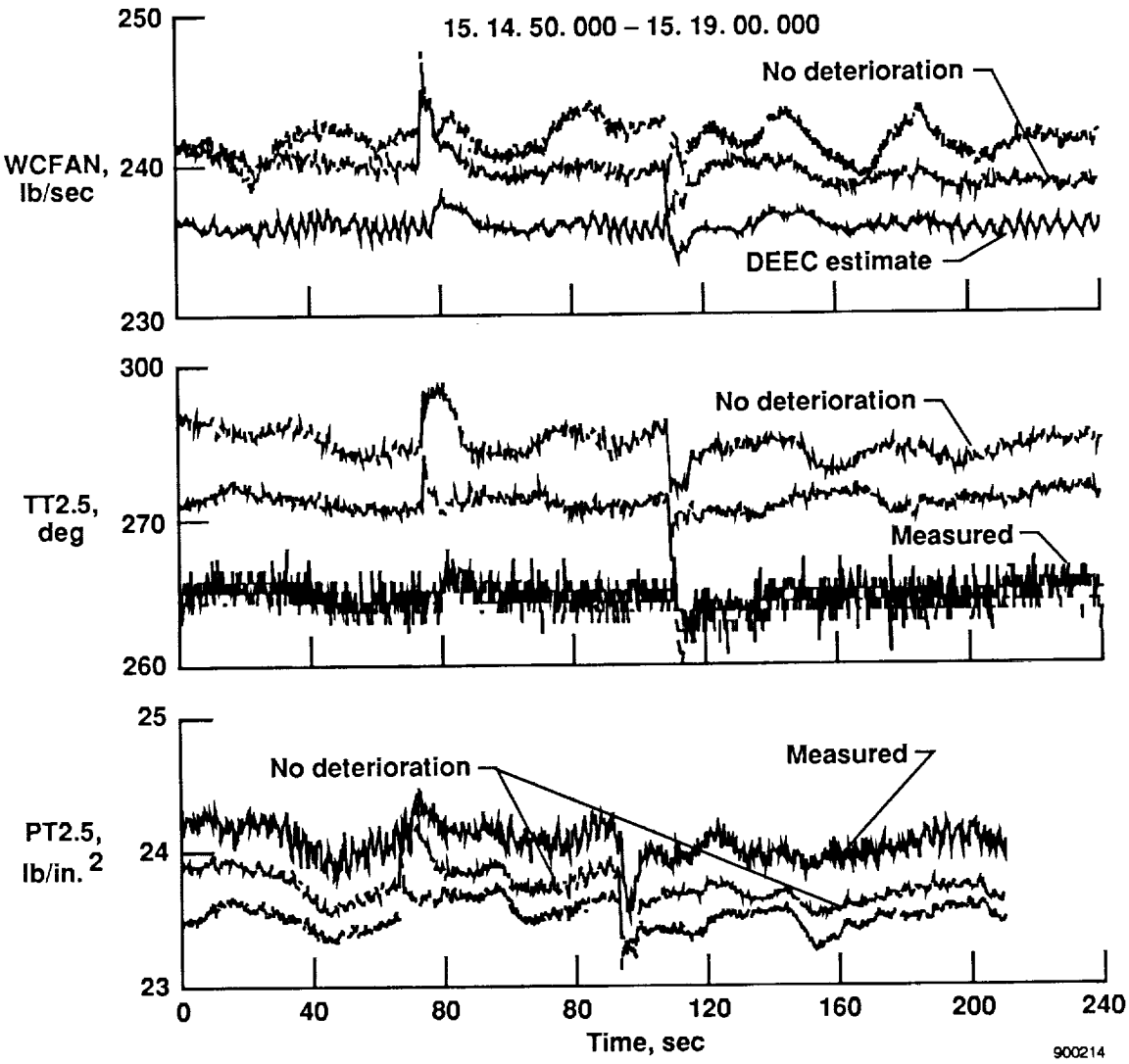

Fig. 17 Comparison of CEM estimates (with and without accounting for deterioration with flight measurements not used in the Kalman filter estimator for PLA = 83°.

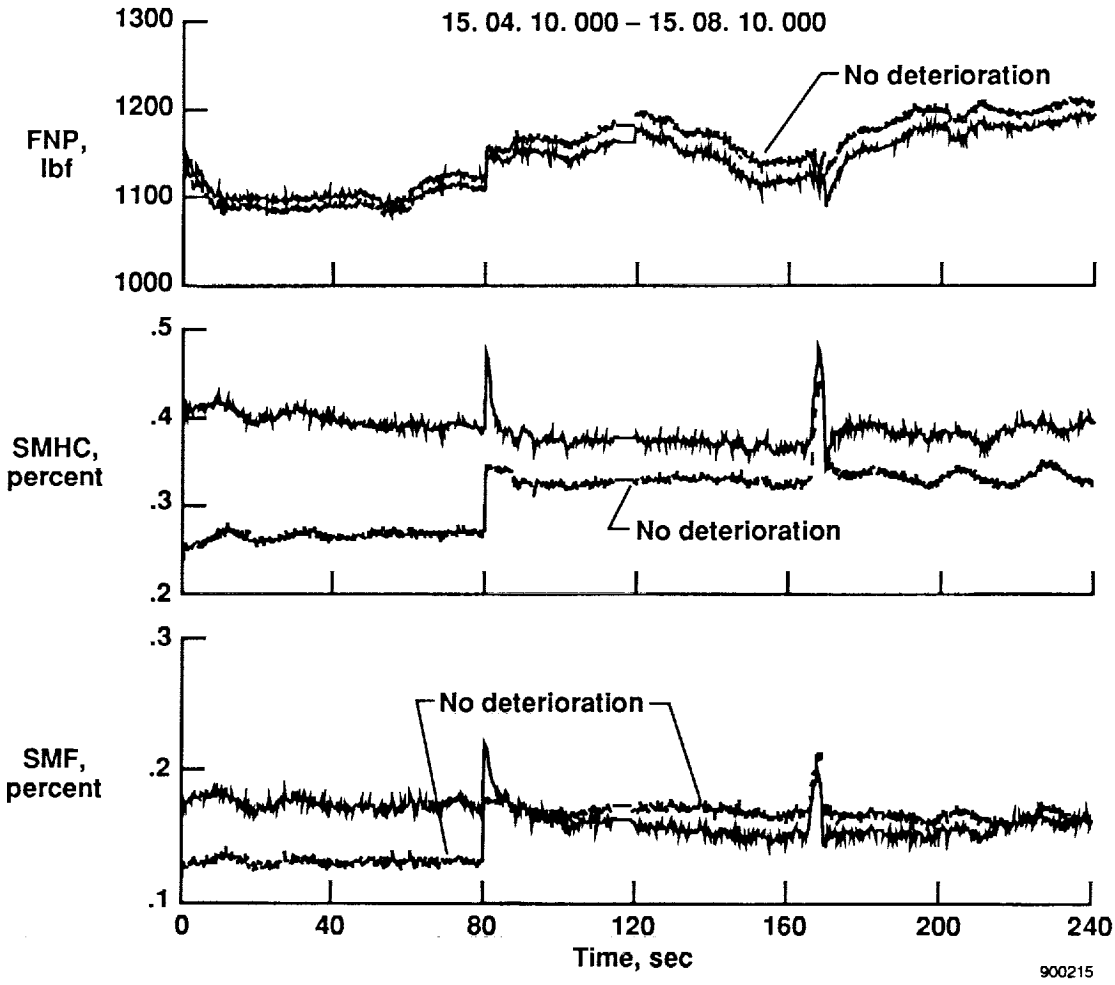

Fig. 18 Sensitivity of CEM estimates to deterioration parameters for PLA = 32°.

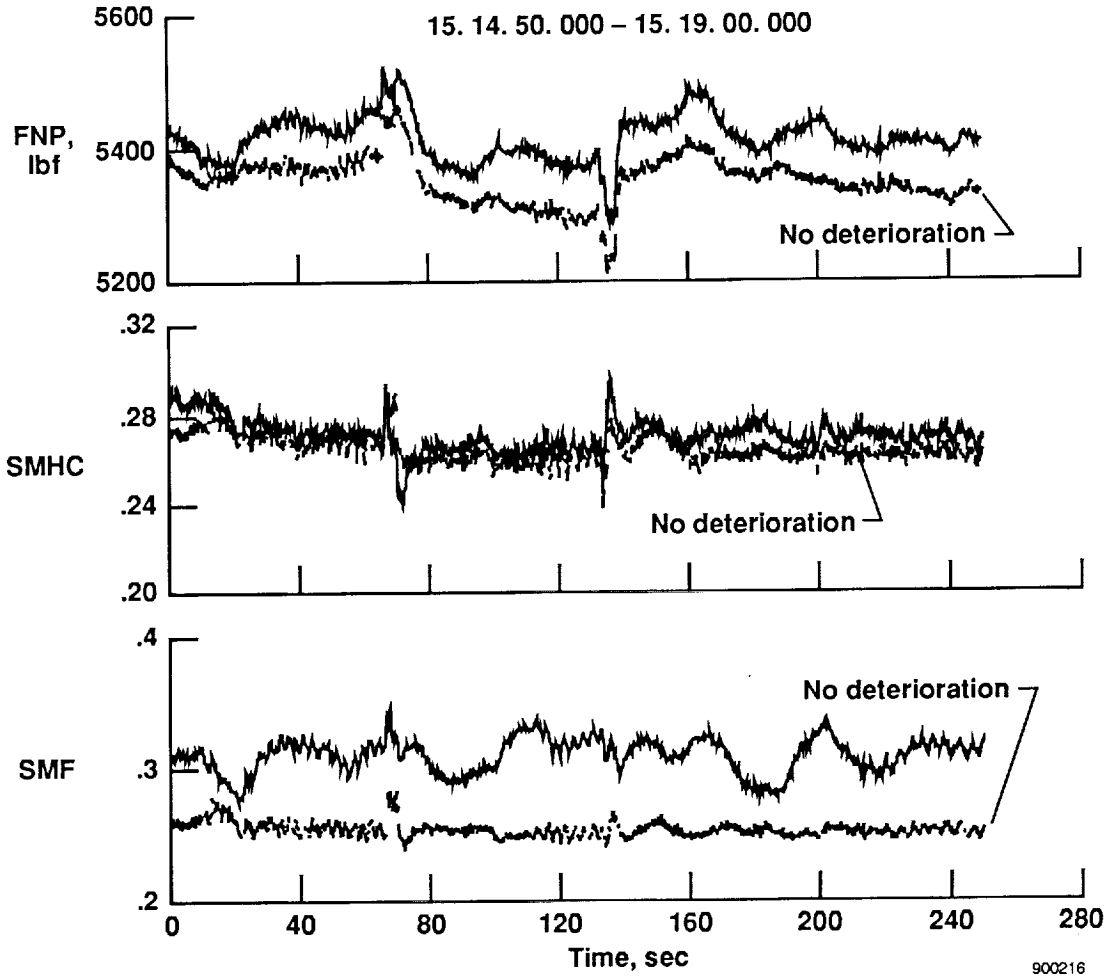

Fig. 19 Sensitivity of CEM estimates to deterioration parameters for PLA = 83°.

NASA
National Aeronautics and Space Administration

Report Documentation Page

1. Report No.	2. Government Accession No.	3. Recipient's Catalog No.
NASA TM-4216		

4. Title and Subtitle

A Preliminary Evaluation of an F100 Engine Parameter Estimation Process Using Flight Data

5. Report Date

August 1990

6. Performing Organization Code

7. Author(s)

Trindel A. Maine, Glenn B. Gilyard, and Heather H. Lambert

8. Performing Organization Report No.

H-1602

10. Work Unit No.

RTOP 505-63-31

9. Performing Organization Name and Address

NASA Ames Research Center
Dryden Flight Research Facility
P.O. Box 273, Edwards, CA 93523-0273

11. Contract or Grant No.

13. Type of Report and Period Covered

Technical Memorandum

12. Sponsoring Agency Name and Address

National Aeronautics and Space Administration
Washington, DC 20546-0001

14. Sponsoring Agency Code

15. Supplementary Notes

Prepared as a paper presented at the AIAA 26th Joint Propulsion Conference, July 16–18, 1990, Orlando, Florida.

16. Abstract

The increasing use of digital engine control allows significant improvement in the performance of aircraft engines. This improvement can be achieved by the use of sophisticated control algorithms designed to recover the full performance potential of the propulsion system. The NASA Ames Research Center, Dryden Flight Research Facility; McDonnell Aircraft Company; and Pratt & Whitney are in the process of developing and flight testing a performance seeking control (PSC) system on the NASA F-15 research aircraft to optimize the near-steady-state performance of the F100 turbofan based propulsion system. The paper is a preliminary evaluation of the engine parameter estimation algorithm which is the primary adaptive element of the PSC algorithm. An evaluation has been made using flight data from the F-15 airplane. The flight data presented were obtained at Mach 0.90 and 30,000 ft and at three throttle positions, one of which was at intermediate power. Based on the theoretical formulation and the limited evaluation using flight data, it appears that this estimation algorithm can provide reasonable estimates of an extended set of engine variables needed for advanced propulsion control law development. However, it must be noted that conclusions drawn from this investigation are not strong because of a lack of independent flight measurements of many of the variables being estimated. Additional sensors or independently derived estimates of many of the extended variables are needed to firmly establish the validity of the estimation algorithm.

17. Key Words (Suggested by Author(s))	18. Distribution Statement
Engine parameter estimation, F-15, Kalman filter, performance seeking control, propulsion system	Unclassified-Unlimited Subject Category - 34

19. Security Classif. (of this report)	20. Security Classif. (of this page)	21. No. of Pages	22. Price
Unclassified	Unclassified	29	A03

NASA FORM 1626 OCT 86

For sale by the National Technical Information Service, Springfield, Virginia 22161

NASA-Langley, 1990